MICROCOPY RESOLUTION TEST CHART

NATIONAL BUREAU OF STANDARDS-1963-A

BACKSCATTERING FROM ANISOTROPIC RANDOM MEDIA

Stanford P. Yukon

DTIC
MAY 1 0 1983

H

ROME AIR DEVELOPMENT CENTER
Air Force Systems Command
Griffiss Air Force Base, NY 13441

83 05 10- 001

This report has been reviewed by the RADC Public Affairs Office (PA) and is releasable to the National Technical Information Service (NTIS). At NTIS it will be releasable to the general public, including foreign nations.

RADC-TR-82-287 has been reviewed and is approved for publication.

APPROVED: *Terence J. Elkins*

TERENCE J. ELKINS
Chief, Propagation Branch
Electromagnetic Sciences Division

APPROVED: *Allan C. Schell*

ALLAN C. SCHELL
Chief, Electromagnetic Sciences Division

FOR THE COMMANDER: *John P. Huss*

JOHN P. HUSS
Acting Chief, Plans Office

SECURITY CLASSIFICATION OF THIS PAGE (When Data Entered)

REPORT DOCUMENTATION PAGE		READ INSTRUCTIONS BEFORE COMPLETING FORM
1 REPORT NUMBER RADC-TR-82-287	2 GOVT ACCESSION NO. AD A278 73	3 RECIPIENT'S CATALOG NUMBER
4 TITLE (and Subtitle) BACKSCATTERING FROM ANISOTROPIC RANDOM MEDIA		5 TYPE OF REPORT & PERIOD COVERED In-House
		6 PERFORMING ORG. REPORT NUMBER
7 AUTHOR(s) Stanford P. Yukon		8 CONTRACT OR GRANT NUMBER(s)
9 PERFORMING ORGANIZATION NAME AND ADDRESS Electromagnetic Sciences Division (EEPI) Hanscom AFB Massachusetts 01731		10 PROGRAM ELEMENT PROJECT TASK AREA & WORK UNIT NUMBERS 61102F 46001608
11 CONTROLLING OFFICE NAME AND ADDRESS Electromagnetic Sciences Division (RADC/EEPI) Hanscom AFB Massachusetts 01731		12 REPORT DATE November 1982
		13 NUMBER OF PAGES 85
14 MONITORING AGENCY NAME & ADDRESS (if different from Controlling Office)		15 SECURITY CLASS (of this report) Unclassified
		15a DECLASSIFICATION DOWNGRADING SCHEDULE

16 DISTRIBUTION STATEMENT (of this Report)

Approved for public release; distribution unlimited.

17 DISTRIBUTION STATEMENT (of the abstract entered in Block 20, if different from Report)

18 SUPPLEMENTARY NOTES

RADC Project Engineer: Stanford P. Yukon, RADC/EEPI

19 KEY WORDS (Continue on reverse side if necessary and identify by block number)

Backscatter	Propagation
Cross section	Anisotropic
Scattering	Green's function
Random media	

20 ABSTRACT (Continue on reverse side if necessary and identify by block number)

The cross section for backscattering from an anisotropic random dielectric medium is computed for the case where the wavelength is much smaller than the outer scale length of the medium and where the path length through the medium can be many times the mean free path for small-angle forward scattering. The cross section as a function of K_i and K_f, the initial and final wavevectors, is obtained by an extension of the cumulative forward-scatter single-backscatter calculation of DeWolf. The cross section for the general
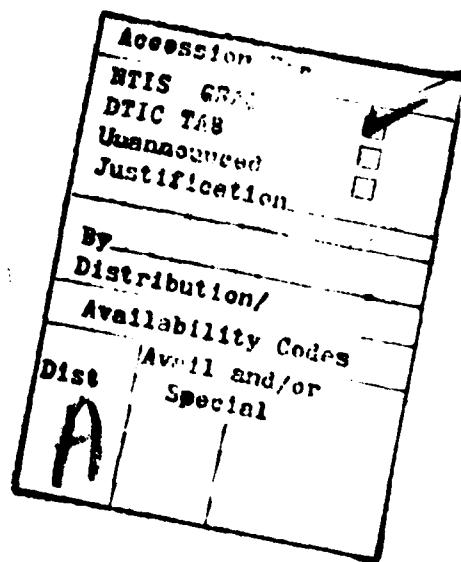
DD FORM 1473 EDITION OF 1 NOV 65 IS OBSOLETE

20. Abstract - Contd.

case is computed by expanding the general expression for the cross section in terms of path dependent correlation functions using Kubo's cumulant expansion method. Evaluation of the resulting Fourier transform is achieved by a functional Taylor Series expansion in terms of multiple convolutions of the projected correlation functions. Numerical results are obtained for the case of a Gaussian correlation function and a method is presented for calculating the cross section for the Kolmogoroff spectrum.

Accession

NTIS GRA

DTIC TAB

Unannounced ☐

Justification ☐

By

Distribution/

Availability Codes

Dist   Avail and/or
        Special

A

Contents

Illustrations

Backscattering From Anisotropic Random Media

1. INTRODUCTION

In this report we formulate a method for determining the backscattering cross section for electromagnetic (as well as a acoustic) waves from slowly-varying anisotropic fluctuations in a random medium. In the electromagnetic case random media having these properties are found in the auroral ionosphere in the form of striations, that is, turbulent plasma that has become elongated into thin columns aligned along the direction of the Earth's magnetic field. Similar structures have also been induced artificially by barium (Ba) releases in the ionosphere above 150 km[1,2] and by high-intensity ionospheric heaters,[3,4] The method developed here is based on the cumulative forward-scatter single-backscatter approximation of De Wolf,[5] extended to include anisotropic media as well as backscattering into (and from) arbitrary directions.

De Wolf employed a perturbation expansion of the Green's function for the electromagnetic wave from which the scattered field and cross section can be determined by an infinite summation of selected (bubble) Feynman diagrams, which arise upon averaging over the fluctuation spectrum. The diagram technique for averaged quantities is analogous to that employed in quantum field theory for

vacuum expectation values with the correlation of two fluctuations replacing the boson propagator. In the method developed here, we bypass the diagrammatic perturbation approach and employ an operator representation[6] for the full Green's function in an arbitrary external field. In this approach the fluctuating field appears in the exponent and the averaging of the product of such exponents to form the expression for the scattered power is reexpressed in terms of correlation functions by utilizing Kubo's cumulant expansion method.[7]

Actual calculation of the cross section for a given turbulence spectrum requires the Fourier transform of an expression involving path dependent projections of correlation functions. To effect this Fourier transform we utilize a technique, similar to that used previously in the calculation of multiphonon absorption,[8] which involves expanding the expression to be Fourier transformed in a functional Taylor series in powers of the projected correlation functions. The subsequent Fourier transform of each term can then be carried out in a straightforward way as a multiple convolution of the projected correlation functions.

Calculation of the backscattering cross section has been carried out for the case of a Gaussian correlation function, where the integrals involved may be evaluated analytically. The results are displayed as graphs of the scattering cross section vs. scattering angle for various choices of scale lengths and thickness for the random media, and angles of incidence and frequency for the incoming wave. A method is also outlined for numerically evaluating the cross section for the case of the more physical Kolmogoroff spectrum, which essentially involves representing the power law correlation function as a sum of Gaussians.

2. MULTISCATTERING FROM A RANDOM ANISOTROPIC MEDIUM

In order to calculate the cross section for backscattering from slowly-varying random fluctuations in a dielectric medium, we will initially assume that depolarization effects are small and that propagation through the medium can be described by the scalar wave equation. Denoting the propagating $\vec{E}$ field by

$$\vec{E}(\vec{r}, t) = \vec{E}(\vec{r}) \, e^{i\omega t - i\vec{k} \cdot \vec{r}} \tag{1}$$

6. Fradkin, E.S. (1966) Application of functional methods in quantum field theory and quantum statistics (II), Nucl. Phys. 76:588.

7. Kubo, R. (1962) Generalized cumulant expansion method, J. Phys. Soc. Japan 17:1100.

8. Bendow, B., Yukon, S.P., and Ying, S.C. (1974) Theory of multiphonon absorption due to nonlinear electric moments in crystals, Phys. Rev. B. 10:2286.

the wave equation for a given transverse component E may be written as

$$\nabla^2 E(\vec{r}) + k^2 \varepsilon(\vec{r}) E(\vec{r}) = 0 \quad . \tag{2}$$

The dielectric permittivity $\varepsilon(\vec{r})$ is taken to be equal to $\langle \varepsilon \rangle$ outside the scattering volume and equal to $\varepsilon(\vec{r}) = \langle \varepsilon \rangle + \delta\varepsilon(\vec{r})$ inside. The scattering volume, as indicated in Figure 1, has been taken to be a slab of infinite extent in the transverse y-z plane and of depth L in the direction of forward propagation, which is taken to be the +x direction.
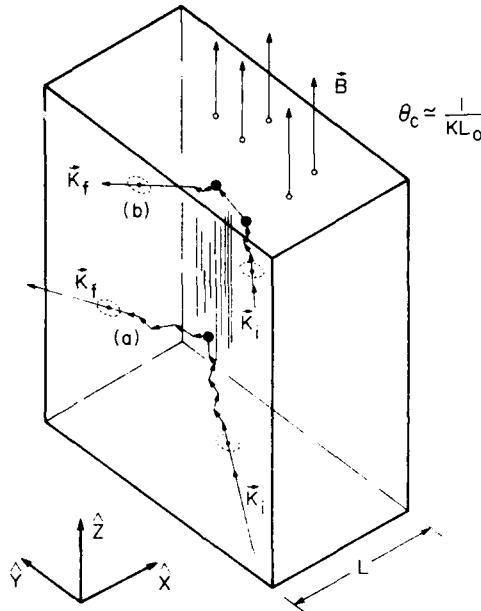
Figure 1. Multiple Small Angle.
Single large angle scattering
event (a) and double large angle
scattering event (b)

In the following we neglect the contribution of reflections and backscattering from the interfaces and consider only backscattering from random fluctuations within the slab volume. We will be interested in calculating scattering from irregularities that tend to be aligned along a given direction such as a background magnetic field $\vec{B}$ (as indicated in Figure 1). We will continue, however, to assume that the fluctuations can be described by a scalar, albeit one that is in general anisotropic.

The goal of the present calculation is to determine the power scattered out of an incoming plane wave beam of unit intensity and arbitrary direction of incidence $\hat{K}_i$ into the scattering direction $\hat{K}_f$, which is also arbitrary. The definition of the angles determining $\hat{K}_i$ and $\hat{K}_f$ is indicated in Figure 2. Following De Wolf[3] we calculate the backscattering cross section on the assumption that the scattering processes that dominate are those composed of a single large-angle hard scattering event followed (and preceded) by multiple small-angle forward scatterings as indicated in Figure 1(a). A calculation of the ratio of power scattered outside a cone of apex angle $2\chi_c$ to that inside yields,[5] in the Born approximation,

$$I(\chi > \chi_c)/I(\chi < \chi_c) = (2k_o L_o \sin (\chi_c/2))^{-5/3} \quad , \tag{3}$$

where $k_o = \omega/c$, and L_o is the macroscale of an assumed 3-D Kolmogoroff spectrum of turbulence. This result indicates that as χ_c increases beyond the small angle $(k_o L_o)^{-1}$, the portion of the incident beam scattered through large angles becomes very small. A similar calculation for the two hard scatter processes of Figure 1(b) yields

$$I(\chi > \chi_c)/I(\chi < \chi_c) \simeq (2k_o L_o \sin (\chi_c/2))^{-8/3} \tag{4}$$

with even smaller ratios for high order processes. Thus, for wavelengths such that $k_o L_o \geq 1$, only the single hard scatter-multiple small angle scattering processes similar to Figure 1(a) need be considered.

We define the scattered wave δE_s as the difference between the field at a given point $\vec{r}$ with fluctuations present, minus the field in their absence. Using the Green's function G for the perturbed medium that satisfies

$$\left[\vec{\nabla}^2 + \frac{\omega^2}{c^2} (\langle \epsilon \rangle + \delta\epsilon(\vec{r})) \right] G(\vec{r} - \vec{r}') = \delta(\vec{r} - \vec{r}') \tag{5}$$

and for the unperturbed medium

$$\left[\vec{\nabla}^2 + \frac{\omega^2}{c^2} \langle \epsilon \rangle \right] G^0(\vec{r} - \vec{r}') = \delta(\vec{r} - \vec{r}') \tag{6}$$

we may express the scattered wave as

$$\delta E_s(\vec{r}) = \int d\vec{r}' [G(\vec{r} - \vec{r}') - G^0(\vec{r} - \vec{r}')] f(\vec{r}') \quad , \tag{7}$$

14
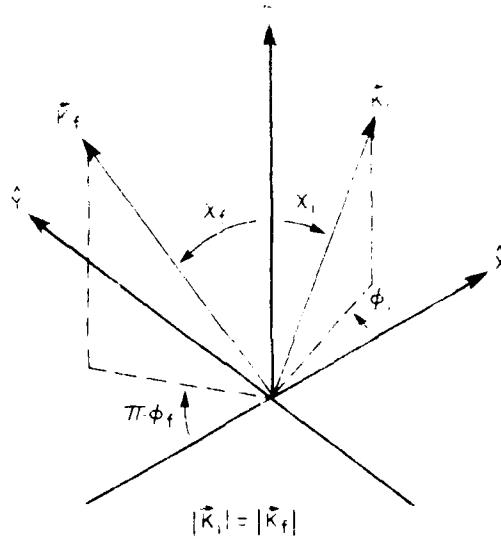
Figure 2. Geometry of Initial and Final
Scattering Angles

where $f(\vec{r})$ is some arbitrary source distribution. The full Green's function may be expanded in terms of G^O and $\delta\varepsilon$ as

$$G = G^O + \sum_{n=1}^{\infty} G^O \cdot \left[-\frac{\omega^2}{c^2} \delta\varepsilon \, G^O \right]^n . \tag{8}$$

The expression for δE_s may thus be written for a delta function source at $\vec{R}_o$ as

$$\delta E_s(\vec{r}) = G(\vec{r}, \vec{R}_o) - G^O(\vec{r}, \vec{R}_o)$$

$$= \sum_{n=1}^{\infty} G^O \left[-\frac{\omega^2}{c^2} \delta\varepsilon \, G^O \right]^n$$

$$= \int d\vec{r}\,' G^O(\vec{r}, \vec{r}\,') \left[-\frac{\omega^2}{c^2} \delta\varepsilon(\vec{r}\,') G^O(\vec{r}\,', \vec{R}_o) \right] +$$

11

$$+ \iint d\vec{r}\,' \, d\vec{r}\,'' \; G^O(\vec{r}, \vec{r}\,') \left[-\frac{\omega^2}{c^2} \, \delta\epsilon(\vec{r}\,') G^O(\vec{r}\,', \vec{r}\,'') \right]$$

$$\cdot \left[-\frac{\omega^2}{c^2} \, \delta\epsilon(\vec{r}\,'') G^O(\vec{r}\,'', \vec{R}_o) \right] + \cdots$$

$$= \int d\vec{r}\,' \, G(\vec{r}, \vec{r}\,') \left(-\frac{\omega^2}{c^2} \, \delta\epsilon(\vec{r}\,') \right) G^O(\vec{r}\,', \vec{R}_o) \quad . \tag{9}$$

For the single large angle-multiple small angle scattering processes of Figure 1(a), the series of Eq. (9) may be rearranged to give

$$\delta E_s(\vec{R}) = \int G_f(\vec{R}, \vec{r}\,') \left(-\frac{\omega^2}{c^2} \, \delta\epsilon(\vec{r}\,') \right) G_i(\vec{r}\,', \vec{R}_o) \, d\vec{r}\,' \quad , \tag{10}$$

where G_i, G_f are the full Green's functions for propagation along $\vec{K}_i$ and $\vec{K}_f$ in the multiple small-angle scatter approximation.

If $\delta\epsilon$ is assumed to be a normally distributed random field with zero mean, averaging Eq. (8) leads to the Dyson equation for the averaged Green's function $\langle G \rangle$

$$\langle G \rangle = G^O + G^O Q \langle G \rangle \tag{11}$$

where Q is the mass operator. In terms of Feynman diagram's, Q is represented by the sum of all strongly-connected diagrams[9]

$$Q = \overset{\frown}{} + \overset{\frown}{} + \overset{\frown}{} + --- \tag{12}$$

where

$$\underset{\vec{r} \qquad \vec{r}\,'}{\cdots\cdots\cdots} = k^4 \, \langle \delta\epsilon(\vec{r}) \, \delta\epsilon(\vec{r}\,') \rangle \quad \text{and} \quad \underset{\vec{r} \qquad \vec{r}\,'}{\text{———}} = G^O(\vec{r}, \vec{r}\,') \quad .$$

The wave number shift, $\delta k^2 = k^2 - k_o^2$, due to the random fluctuations is then given by the Fourier transform of the mass operator Q as

9. Tatarskii, V.I. (1971) The effect of the turbulent atmosphere on wave propagation, Israel Program for Scientific Translations, Jerusalem.

12

$$\delta k^2 = \int e^{i\vec{k}\cdot\vec{r}} Q(\vec{r}) d\vec{r} \quad . \tag{13}$$

To lowest order in $\delta\varepsilon$ only the first diagram in Eq. (12) is retained. Assuming a simple exponential for the correlation function

$$\langle \delta\varepsilon(\vec{r}) \delta\varepsilon(\vec{r}') \rangle = \delta\varepsilon^2 e^{-|\vec{r}-\vec{r}'|/\ell} \tag{14}$$

leads to the dispersion relation[9]

$$k^2 - k_o^2 = \frac{\delta\varepsilon^2 k_o^4 \ell^2}{[k^2\ell^2 + (1 - ik_o\ell)^2]} \quad . \tag{15}$$

To lowest order in $\delta\varepsilon$, for $k_o\ell \geq 1$ this gives

$$Re(\delta k) = \frac{-k_o \delta\varepsilon^2}{8} \quad , \qquad Im(\delta k) = \frac{\delta\varepsilon^2 k_o^2 \ell}{4} \quad , \tag{16}$$

thus there will be both a wave number shift as well as attenuation due to multiple scattering in the random medium. As an example, a 30-MHz signal traversing a random medium with 1 percent permittivity fluctuations having a 100-m scale length would experience a wave number shift $\frac{\delta k}{k} = 1.25 \times 10^{-3}$ and an attenuation of $\alpha = 1.0/km$.

To calculate the scatter cross section in the Born approximation, we approximate G_i, G_f by G^o, where

$$G^o(\vec{r}, \vec{r}') = \frac{1}{4\pi} \frac{e^{ik|\vec{r}-\vec{r}'|}}{|r - r'|} \quad . \tag{17}$$

The expression for the scattered field at $\vec{R}$ for a delta function source at $\vec{R}_o$ given by Eq. (10) may then be written as

$$\delta E_s^o(\vec{R}) = \int d\vec{r}' G^o(\vec{R}, \vec{r}')(-k^2 \delta\varepsilon(\vec{r}')) G^o(\vec{r}', \vec{R}_o) \quad . \tag{18}$$

13

In the plane wave limit $(\vec{R}_s, \vec{R}_i \to \infty)$ we may approximate

$$|\vec{R} - \vec{r}'| \simeq R - \vec{r}' \cdot \hat{R} \quad .$$

Expanding G^o to lowest order in r/R_o yields

$$G^o(\vec{R}, \vec{r}') \simeq \frac{1}{4\pi R} e^{+ikR - ik\vec{r}' \cdot \hat{R}} = \frac{e^{+ikR - i\vec{K}_f \cdot \vec{r}'}}{4\pi R}$$

and

$$G^o(\vec{r}', \vec{R}_o) = \frac{1}{4\pi R_o} e^{ikR_o + i\vec{K}_i \cdot \vec{r}'} \quad . \tag{20}$$

The scattering cross section may now be determined by dividing the power scattered into a given direction by the power in the incident beam. In the plane wave limit the cross section deduced from δE_s is given by

$$\sigma_{\vec{K}_i, \vec{K}_f} = 4\pi \left\langle \left| f_{\vec{K}_i, \vec{K}_f} \right|^2 \right\rangle \quad , \tag{21}$$

where the average is taken over the distribution of random density fluctuations, and $f_{\vec{K}_i, \vec{K}_f}$ the scattering amplitude is defined through

$$f_{\vec{K}_i, \vec{K}_f} = \lim_{R_o, R \to \infty} \left\{ 4\pi R R_o e^{-ik(R + R_o)} \delta E_s(\vec{R}) \right\} \quad . \tag{22}$$

Reintroducing the vector character of the field $\delta \vec{E}_s$ would lead to a vector scattering amplitude

$$\vec{f}_{\vec{K}_i, \vec{K}_f} = (-\hat{K}_f \times \hat{K}_f \times \hat{E}_0) f_{\vec{K}_i, \vec{K}_f}$$

and a cross section[9]

$$\sigma_v(\vec{K}_i, \vec{K}_f) = \sigma_{\vec{K}_i, \vec{K}_f} \cdot \sin^2(\psi) \quad , \tag{23}$$

14

where ι is the angle between the polarization direction of the incident wave $\vec{E}_0$ and the scattering direction $\vec{K}_f$. In what follows we shall leave off the $\sin^2(\iota)$ polarization dependence and consider only the scalar quantities $f_{\vec{K}_i, \vec{K}_f}$ and $\sigma_{\vec{K}_i, \vec{K}_f}$.

Thus, for the Born approximation we have

$$f_{\vec{K}_i, \vec{K}_f} = \frac{K^2}{4\pi} \int d\vec{r}\,' \, e^{i(\vec{K}_i - \vec{K}_f)\cdot \vec{r}\,'} \, \delta\epsilon(\vec{r}\,') \tag{24}$$

and

$$\sigma_{\vec{K}_i, \vec{K}_f} = \frac{K^4}{4\pi} \int d\vec{r}\,' \int d\vec{r}\,'' \, e^{i(\vec{K}_i - \vec{K}_f)(\vec{r}\,' - \vec{r}\,'')} \, \langle \delta\epsilon(\vec{r}\,') \, \delta\epsilon^*(\vec{r}\,'') \rangle \quad . \tag{25}$$

Changing to new variables $\Delta\vec{r} = \vec{r}\,' - \vec{r}\,''$, $\vec{r} = \dfrac{\vec{r}\,' + \vec{r}\,''}{2}$, and $\Delta\vec{K} = \vec{K}_i - \vec{K}_f$, this may be written as

$$\sigma_{\vec{K}_i, \vec{K}_f} = \frac{K^4}{4\pi} \int d\vec{r} \int d\Delta\vec{r} \, e^{i\Delta\vec{K}\cdot\Delta\vec{r}} \, \langle \delta^2\epsilon(\Delta\vec{r}) \rangle$$

$$= \frac{K^4 \epsilon^2 V}{4\pi} \, \tilde{\Phi}(\Delta\vec{K}) \quad , \tag{26}$$

where $\tilde{\Phi}(\vec{K})$ is the Fourier transform of the correlation function for a homogeneous medium

$$\frac{1}{\epsilon^2} \langle \delta\epsilon^2(\vec{r} - \vec{r}\,') \rangle \equiv \frac{1}{\epsilon^2} \langle \delta\epsilon(\vec{r}) \, \delta\epsilon^*(\vec{r}\,') \rangle \quad . \tag{27}$$

We note that if $\langle \delta\epsilon^2(\Delta\vec{r}) \rangle$ is Gaussian, then $\tilde{\Phi}(\vec{K})$ is also Gaussian. We shall assume that $\tilde{\Phi}$ can be factored as

$$\tilde{\Phi}(K_x, K_y, K_z) = \tilde{d}(K_z) \tilde{\mathscr{D}}(K_x, K_y) \quad . \tag{28}$$

15

The two functional forms that are of greatest interest are the Gaussian

$$\tilde{\Phi}_{\mathcal{G}}(\vec{K}) = \tilde{d}(K_z)\tilde{\mathcal{D}}_{\mathcal{G}}(\vec{K}_\perp) = \left[\sqrt{\pi}\, L_\parallel\, e^{-K_z^2 L_\parallel^2/4}\right]\left[\pi L_\perp^2\, e^{-\vec{K}_\perp^2 L_\perp^2/4}\right] \tag{29}$$

and

$$\tilde{\Phi}_{\mathcal{K}}(\vec{K}) = \tilde{d}(K_z)\tilde{\mathcal{D}}_{\mathcal{K}}(\vec{K}_\perp) = \left[\sqrt{\pi}\, L_\parallel\, e^{-K_z^2 L_\parallel^2/4}\right]\frac{\kappa}{\left[1 + \vec{K}_\perp^2 L_\perp^2\right]^{\mu+1}} \quad , \tag{30}$$

where $\mu = 5/6$ corresponds to the Kolmogoroff spectrum for turbulence. In the following we shall assume that $L_\parallel > L_\perp$.

To include multiscattering effects in the simplest way we utilize the eikonal approximation[9] for G given by

$$G(\vec{r}, \vec{r}\,') = G^0(\vec{r}, \vec{r}\,')\, e^{i\frac{K}{2}\int_{-\infty}^{S}\delta\epsilon(\vec{r}+s'\hat{K})ds'} \quad , \tag{31}$$

where the integral is to be taken over the effective path length in the medium. If we restrict the possible scattering angles to those outside a small cone of half angle $\theta_c = (k_o L_o)^{-1}$ around the direct backscatter direction $(\vec{K}_f = -\vec{K}_i)$ then the averages over products of G_i and G_f are essentially disjoint and may be factored. Using the eikonal approximation and grouping terms on each path together, we get

$$\sigma_{\vec{K}_i, \vec{K}_f} = \frac{K^4}{4\pi}\int d\vec{r}\,''\int d\vec{r}\,'\, e^{i\Delta\vec{K}\cdot(\vec{r}\,'-\vec{r}\,'')}$$

$$\times \left\langle e^{i\frac{K}{2}\int_{-\infty}^{S'}\delta\epsilon(\vec{r}\,'+\sigma\hat{K}_i)d\sigma}\; e^{-i\frac{K}{2}\int_{-\infty}^{S''}\delta\epsilon^*(\vec{r}\,''+\sigma'\hat{K}_i)d\sigma'}\right\rangle$$

$$\times \langle\delta\epsilon(\vec{r}\,')\,\delta\epsilon^*(\vec{r}\,'')\rangle\left\langle e^{-i\frac{K}{2}\int_{-\infty}^{S'}\delta\epsilon^*(\vec{r}\,'+\sigma\hat{K}_f)d\sigma}\; e^{+i\frac{K}{2}\int_{-\infty}^{S''}\delta\epsilon(\vec{r}\,''+\sigma'\hat{K}_f)d\sigma'}\right\rangle \; , \tag{32}$$

16

where we have made the further assumption that the correlation between ... of the hard scattering fluctuations $\langle \delta\varepsilon(\vec{r}') \delta\varepsilon^*(\vec{r}'') \rangle$ may be factored out as well.

We now use Kubo's cumulant expansion[7]

$$\left\langle \sum_{j=1}^{N} \xi_j^{(\lambda)} \right\rangle_c \quad \left\langle \left(\sum_{j=1}^{N} \xi_j^{(\lambda)} \right)_c - 1 \right\rangle \tag{ }$$

where the subscript c indicates that a cumulant average is to be taken ... The lowest order cumulants are defined as

$$\langle \xi_j \rangle_c = \langle \xi_j \rangle$$

$$\langle \xi_j^2 \rangle_c = \langle \xi_j^2 \rangle - \langle \xi_j \rangle^2$$

$$\langle \xi_j \xi_k \rangle_c = \langle \xi_j \xi_k \rangle - \langle \xi_j \rangle \langle \xi_k \rangle$$

For the case under consideration, $\xi = ...$ and we obtain for the ... along $\vec{k}$,

$$ ... $$

$$ ... $$

where we have truncated the cumulant expansion, keeping terms up to and quadratic. Changing variable to ...

$$\frac{1}{2} s_i \int d\tau [\langle \varepsilon'(\Delta\vec{r} + \hat{k}_i \tau)^2 \rangle - \langle \varepsilon'(0, ...) \rangle] \tag{ }$$

where s_i is the path length in the medium along $\hat{k}_i$ to the scatter site $\vec{r} = \frac{\vec{r}' + \vec{r}''}{2}$. Integration along the path length $\hat{k}_i \cdot \tau$ has the effect of changing the 3-D correlation function into an effective 2-D correlation function in the plane transverse to $\hat{k}_i$ or $\hat{k}_f$. The expression for the multiscatter cross section becomes, changing variable to $\vec{r} = \frac{\vec{r}' + \vec{r}''}{2}$, $\Delta\vec{r} = \vec{r}' - \vec{r}''$

$$\sigma_{\vec{K}_i, \vec{K}_f} = \frac{K^4}{4\pi} \int d\vec{r} \int d\Delta\vec{r}\, e^{i\Delta\vec{K}\cdot\Delta\vec{r}}$$

$$\times\, e^{\frac{K^2 s_i}{4} \int_{-\infty}^{\infty} \{\langle\delta\varepsilon^2(\Delta\vec{r}+\hat{K}_i\tau)\rangle - \langle\delta\varepsilon^2(\hat{K}_i\tau)\rangle\}\,d\tau}$$

$$\times\, \langle\delta\varepsilon^2(\Delta\vec{r})\rangle\, e^{\frac{K^2 s_f}{4}\int_{-\infty}^{\infty}\{\langle\delta\varepsilon^2(\Delta\vec{r}+\hat{K}_f\tau)\rangle - \langle\delta\varepsilon^2(\hat{K}_f\tau)\rangle\}\,d\tau} \qquad (37)$$

We now reexpress the path dependent terms in the exponent in terms of their Fourier transforms as

$$\frac{K^2}{4}\int_{-\infty}^{\infty}\langle\delta\varepsilon^2(\Delta\vec{r}+\hat{K}_i\tau)\rangle\,d\tau$$

$$= \frac{K^2}{4}\int_{-\infty}^{\infty}d\tau\int\frac{d\vec{q}}{(2\pi)^3}\,e^{i\vec{q}\cdot(\Delta\vec{r}+\hat{K}_i\tau)}\,\langle\widetilde{\delta\varepsilon}^2(\vec{q})\rangle$$

$$= \frac{K^2\varepsilon^2}{4}\int\frac{d\vec{q}}{(2\pi)^2}\,e^{i\vec{q}\cdot\Delta\vec{r}}\,\delta(\hat{K}_i\cdot\vec{q})\,\widetilde{P}(\vec{q}) \qquad (38)$$

The delta function $\delta(\hat{K}_i\cdot\vec{q})$ acts as a projection operator, allowing only those values of $\vec{q}$ that lie in the plane perpendicular to $\hat{K}_i$ at the origin to contribute to the Fourier integral. We are thus led to define the (path dependent) projected correlation function $D_i(\Delta\vec{r})$ through the relation

$$\varepsilon^2\, D_i(\Delta\vec{r}) = \frac{K^2}{4}\int_{-\infty}^{\infty}\langle\delta\varepsilon^2(\Delta\vec{r}+\hat{K}_i\tau)\rangle\,d\tau \qquad (39)$$

where the (path dependent) correlation $\langle\ldots\rangle$ is defined as the difference of the projected $\Delta\vec{r}$

$$\alpha_i = \frac{K^2}{8} \int_{-\infty}^{\infty} \langle \delta \epsilon^2(\hat{K}_i \tau) \rangle \, d\tau \quad . \tag{40}$$

(α_i can be shown to be the attenuation due to the random medium for a plane wave propagating in the direction $\hat{K}_i$).

For the Gaussian correlation function of Eq. (29) this leads to an expression for α_i given by

$$\alpha_i = \frac{K^2 \epsilon^2 L_i L_\perp \sqrt{\pi}}{8 \left[\cos^2(\chi) L_i^2 + \sin^2(\chi) L_\perp^2 \right]^{1/2}} \tag{41}$$

thus

$$\alpha_{\chi=0} = \frac{K^2 \epsilon^2 L_\perp \sqrt{\pi}}{8} \qquad \text{and} \qquad \alpha_{\chi=\pi/2} = \frac{K^2 \epsilon^2 L_i \sqrt{\pi}}{8} \quad . \tag{42}$$

Expressing the path length along $\hat{K}_i$ from the $x = 0$ plane to the $x = x$ plane as

$$s(x) = x \cdot \sqrt{\frac{1}{\sin^2(\chi_i)} + \tan^2(\phi_i)} \qquad \text{(see Appendix A)} \tag{43}$$

and defining

$$\beta_i = 2\alpha_i \sqrt{\frac{1}{\sin^2(\chi_i)} + \tan^2(\phi_i)} \quad , \tag{44}$$

the path dependent terms can be written as

$$e^{x\beta_i[D_i(\Delta\vec{r})-1]} \; e^{x\beta_f[D_f(\Delta\vec{r})-1]} \quad . \tag{45}$$

18

Performing the $d\vec{r}$ integration yields

$$A \int_0^L dx \; e^{x\beta_i[D_i(\vec{\Delta r})-1]+x\beta_f[D_f(\vec{\Delta r})-1]}$$

$$= [A \cdot L] \left\{ \frac{e^{L\beta_i[D_i(\vec{\Delta r})-1]+L\beta_f[D_f(\vec{\Delta r})-1]} - 1}{\left[L\beta_i[D_i(\vec{\Delta r}) - 1] + L\beta_f[D_f(\vec{\Delta r}) - 1]\right]} \right\} . \tag{46}$$

The scattering cross section is thus given by the Fourier transform

$$\sigma_{\vec{K}_i, \vec{K}_f} = \frac{K^4}{4\pi} \; V \int d\vec{\Delta r} \; e^{i\vec{\Delta K} \cdot \vec{\Delta r}} \; \langle \delta\epsilon^2(\vec{\Delta r}) \rangle$$

$$\times \left\{ \frac{e^{\{L\beta_i[D_i(\vec{\Delta r})-1] + L\beta_f[D_f(\vec{\Delta r})-1]\}} - 1}{\{L\beta_i[D_i(\vec{\Delta r}) - 1] + L\beta_f[D_f(\vec{\Delta r}) - 1]\}} \right\} . \tag{47}$$

To effect the Fourier transform we define

$$f(\vec{\Delta r}) = \{L\beta_i[D_i(\vec{\Delta r}) - 1] + L\beta_f[D_f(\vec{\Delta r}) - 1]\} \tag{48}$$

and expand $[e^f - 1]/f$ in a double functional Taylor series about $D_i(\vec{\Delta r})$, $D_f(\vec{\Delta r}) = 0$. Each term of the form

$$\int e^{i\vec{K} \cdot \vec{\Delta r}} \; \langle \delta\epsilon^2(\vec{\Delta r}) \rangle \; D_i^{n-j}(\vec{\Delta r}) \; D_f^j(\vec{\Delta r}) \; d\vec{\Delta r} \tag{49}$$

will thus be an $n + 1$ fold convolution where we define the convolution operation by

$$\int d\vec{r} \; e^{i\vec{K} \cdot \vec{r}} \; g_1(\vec{r}) \; g_2(\vec{r}) = \int \frac{d\vec{p}}{(2\pi)^3} \; \tilde{g}_1(\vec{K} - \vec{p}) \; \tilde{g}_2(\vec{p}) \tag{50}$$

and the iterated convolution through

$$\tilde{D}^{n+1}(\vec{K}) = \int \frac{d\vec{p}}{(2\pi)^3} \; \tilde{D}^n(\vec{K} - \vec{p}) \; \tilde{D}(\vec{p}) \quad . \tag{51}$$

The double Taylor series expansion of the functional $[e^f - 1]/f$ about $D_i(\vec{r})$, $D_f(\vec{r}) = 0$ thus yields

$$\sum_{n=0}^{\infty} \sum_{j=0}^{n} \frac{1}{n!} \binom{n}{j} \beta_i^{n-j} \beta_f^j \times \frac{\partial^n}{\partial f^n} \left[\frac{e^f - 1}{f} \right]_{|f=-(\beta_i+\beta_f)L} D_i^{n-j}(\Delta\vec{r}) \; D_f^j(\Delta\vec{r}) \quad . \tag{52}$$

The derivative $\partial_f^n([e^f - 1]/f)_{|f=-x}$ may be expressed in terms of the incomplete gamma function $\gamma(n, x)$, as (see Appendix B)

$$\partial_f^n([e^f - 1])/f)_{|f=-x} = \frac{\gamma(n + 1), \, x)}{x^{n+1}} \quad . \tag{53}$$

The final expression for the scattering cross section for a unit volume is then given by

$$\sigma_{\vec{K}_i, \vec{K}_f} \equiv \sum_{n=0}^{\infty} \sigma_{\vec{K}_i, \vec{K}_f}^{[n]} = \frac{K^4}{4\pi} \int d\Delta\vec{r} \; e^{i\Delta\vec{K}\cdot\Delta\vec{r}} \langle \delta^2_\epsilon (\Delta\vec{r}) \rangle \times$$

$$\times \left\{ \left[\frac{1 - e^{-(\beta_i+\beta_f)L}}{(\beta_i + \beta_f)L} \right] + \sum_{n=1}^{\infty} \sum_{j=0}^{n} \frac{1}{n!} \frac{n!}{(n - j)! \, j!} \times \right.$$

$$\left. \times \beta_i^{n-j} \beta_f^j \cdot \frac{\gamma(n + 1, \, (\beta_i + \beta_f)L)}{L(\beta_i + \beta_f)^{n+1}} \cdot D_i^{n-j}(\Delta\vec{r}) \; D_f^j(\Delta\vec{r}) \right. \quad , \tag{54}$$

where the $n = 0$ term of the infinite sum has been separated out as the first term in the large brackets, and is essentially the Born term modified by the attenuation along the forward and backward paths.

The nth convolution of the projected correlation function defined in Eqs. (38) and (39) is calculated in the most straightforward manner by using the delta function in Eq. (38) to integrate over the $\vec{q}$ coordinate parallel to $\vec{K}_i$ and then developing

the iterated (2-D) convolution series as defined in Eq. (51) in the plane perpendicular to $\vec{K}_i$. This approach runs into difficulties due to the fact that the correlation functions of Eqs. (29) and (30) factor into functions defined along z and the $x-y$ plane rather than $\vec{K}_i$ (or $\vec{K}_f$) and the plane perpendicular to $\vec{K}_i$ (or $\vec{K}_f$). In addition, the general term in the sum of Eq. (54) requires the convolution of $\tilde{D}_i^{n-j}$ and D_f^j, which are defined on planes of differing orientation. The simplest way to avoid both of these difficulties is to use the projection delta functions in Eq. (38) to integrate over the q_z coordinate, projecting both $\tilde{D}_i^{n-j}$ and $\tilde{D}_f^j$ onto the $q_x - q_y$ plane.

To actually calculate a given convolution product it is best to form the $(n-1)^{th}$ convolution of $\tilde{D}_i$ in a coordinate system $\hat{p}_z$, $\hat{p}_\perp$ where $\hat{p}_{\perp 1}$ is directed along $\vec{K}_{i_\perp}$ and where $\vec{K}_{i_\perp}$ is the projection of $\vec{K}_i$ onto the $p_x - p_y$ plane as shown in Figure 3. In a similar manner, the jth convolution of $\tilde{D}_f(\vec{q})$ can be formed in a coordinate system where $\hat{q}_{\perp 1}$ is directed along $\vec{K}_{f_\perp}$.
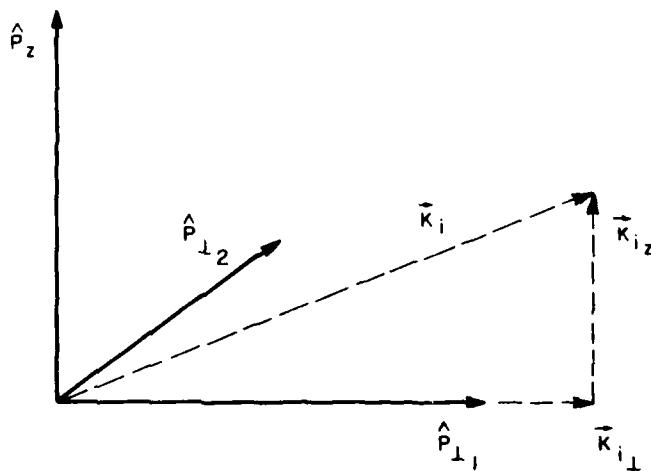
Figure 3. Decomposition of Scattering Wave Vector Into Components Parallel and Perpendicular to Magnetic Field Direction

One can show that the convolution of two $\vec{K}$ projected functions is another $\vec{K}$ projected function (see Appendix C). Thus, for the Gaussian

$$\Phi_{\mathcal{D}}(\vec{p}) = \tilde{d}(p_z L_{\shortparallel})\tilde{\mathcal{D}}_{\mathcal{D}}(\vec{p}_\perp L_\perp) \tag{55}$$

22

we get for the projected correlation function in the $p_x - p_y$ plane a hybrid given by

$$\widetilde{D}_i^{n-j}(\vec{p}) = \check{D}_i^{n-j}(\vec{p}_\perp)[2\pi\delta(\vec{K}_i \cdot \vec{p})K_i \cos(\chi_i)] \tag{56}$$

with

$$\check{D}_i^{n-j}(\vec{p}_\perp) = \frac{\pi L_\perp \widetilde{L}_i}{(n-j)} e^{-p_2^2 L_\perp^2/4(n-j)} e^{-p_1^2 \widetilde{L}_i^2/4(n-j)} \tag{57}$$

where

$$\widetilde{L}_i^2 = L_\perp^2 + L_\parallel^2 \tan^2(\chi_i) . \tag{58}$$

A general term in the sum of Eq. (54) with $(n-j) > 0$, $j > 0$ will require the Fourier transform

$$\int d\Delta\vec{r}\ e^{i\Delta\vec{K}\cdot\Delta\vec{r}} \langle \delta\varepsilon^2(\Delta\vec{r})\rangle D_i^{n-j}(\Delta\vec{r}) D_f^j(\Delta\vec{r}) , \tag{59}$$

which we reexpress as a double convolution

$$\int d\Delta\vec{r}\ e^{i(\vec{K}_i - \vec{K}_f)\cdot\Delta\vec{r}} \int \frac{d\vec{\ell}}{(2\pi)^3} e^{i\vec{\ell}\cdot\Delta\vec{r}} \langle \delta\varepsilon^2(\vec{\ell})\rangle$$

$$\times \int \frac{d\vec{p}}{(2\pi)^3} \widetilde{D}_i^{n-j}(\vec{p}) e^{i\vec{p}\cdot\Delta\vec{r}} \cdot \int \frac{d\vec{q}}{(2\pi)^3} \widetilde{D}_f^j(\vec{q}) e^{i\vec{q}\cdot\Delta\vec{r}}$$

$$= \int \frac{d\vec{p}\,d\vec{q}\,d\vec{\ell}}{(2\pi)^6} \langle \delta\varepsilon^2(\vec{\ell})\rangle \widetilde{D}_i^{n-j}(\vec{p}) \widetilde{D}_f^j(\vec{q}) \delta(\vec{\ell} + \vec{p} + \vec{q} + \vec{K}_i - \vec{K}_f) . \tag{60}$$

Changing variables to $\vec{p}\,' = \vec{p} + \vec{K}_i$, $\vec{q}\,' + -\vec{q} + \vec{K}_f$ and dropping primes this becomes after integration over $d\vec{\ell}$

$$\int \frac{d\vec{p}\, d\vec{q}}{(2\pi)^6} \langle \widetilde{\delta\epsilon}^2(\vec{q}' - \vec{p}')\rangle \, \widetilde{D}_i^{n-j}(\vec{p}' - \vec{K}_i) \, \widetilde{D}_f^j(\vec{K}_f - \vec{q}')$$

$$= \int \frac{d\vec{p}\, d\vec{q}}{(2\pi)^6} \langle \widetilde{\delta\epsilon}^2(\vec{q} - \vec{p})\rangle \, \overset{\vee}{D}_i^{n-j}(\vec{p}_\perp - \vec{K}_{i\perp}) \, \overset{\vee}{D}_f^j(\vec{K}_{f\perp} - \vec{q}_\perp)$$

$$\times \delta\left((\vec{p} - \vec{K}_i) \cdot \vec{K}_i\right) \cdot \delta\left((\vec{q} - \vec{K}_f) \cdot \vec{K}_f\right) (2\pi K_{iz})(2\pi K_{fz}) \quad . \tag{61}$$

This can now be evaluated by integrating the two delta functions over p_z and q_z and projecting $\vec{q}_\perp$ along the $\vec{p}_\perp$ axes as

$$\hat{p}_1 \cdot [\vec{q}_\perp] = q_1 \cos(\phi_f - \phi_i) - q_2 \sin(\phi_f - \phi_i)$$

$$\hat{p}_2 \cdot [\vec{q}_\perp] = q_1 \sin(\phi_f - \phi_i) + q_2 \cos(\phi_f - \phi_i) \tag{62}$$

to form the argument for $\langle \widetilde{\delta\epsilon}^2(\vec{q} - \vec{p})\rangle$. These operations are carried out in Appendix D for the Gaussian correlation function of Eq. (29).

The terms in the sum of Eq. (54) with $(n - j) = 0$, $j > 0$, and $(n - j) > 0$, $j = 0$ can be evaluated in a similar manner. Results for the Gaussian correlation function are developed in Appendix E. The expression for the total cross section for the Gaussian correlation function, using the results of Appendices D and E, thus becomes a simple double sum of exponentials. This expression has been evaluated for various values of the medium parameters $L_\perp$, $L_\parallel$, slab thickness L, wave number K, and angle of incidence χ_i (and is plotted in Figures 6a through 11e). The behavior of the cross section for the Gaussian correlation function is discussed in the next section.

The evaluation of the cross section given by Eq. (54) for the Kolmogoroff spectrum of Eq. (30) is more difficult due to the fact that integration of the projection delta function of Eq. (38) over p_z leads to an expression for $D[\vec{K}]$ which, as in the Gaussian case, is no longer a function of $p_\perp^2$ but of $p_{\perp 1}$ and $p_{\perp 2}$ separately and which, moreover, does not factor as does the Gaussian. The 2-D convolutions for $D[\vec{K}]$ can be carried out numerically in a straightforward way with no difficulty other than that of the computation time and core memory involved. Since the series of Eq. (54) converges rapidly (N = 5 is sufficient for the Gaussian) this is not a severe problem unless a large number of points (for example, as represented by the curves of Figures 6a through 11e), are involved. In order to compute $\sigma_{\text{(...)}}$ for

the Kolmogoroff spectrum in a more economical way, we represent the correlation function

$$\tilde{\mathcal{B}}_{\mathcal{K}}(\vec{q}_{\perp}^{\,2}) = \frac{\kappa}{\left[1 + \vec{q}_{\perp}^{\,2}\, L_{\perp}^{2}\right]^{\nu}} \tag{63}$$

as a sum of Gaussians by employing the integral representation for the gamma function

$$\Gamma(\nu) = \Lambda^{\nu} \int_{0}^{\infty} X^{\nu-1}\, e^{-\Lambda x}\, dx \quad . \tag{64}$$

Letting $\Lambda = \left[1 + \vec{q}_{\perp}^{\,2}\, L_{\perp}^{2}\right]$, this yields

$$\frac{1}{\left[1 + \vec{q}_{\perp}^{\,2}\, L_{\perp}^{2}\right]^{\nu}} = \frac{1}{\Gamma(\nu)} \int_{0}^{\infty} x^{\nu-1}\, e^{-x}\, e^{-\vec{q}_{\perp}^{\,2}\, L_{\perp}^{2}\, x}\, dx$$

$$= \frac{1}{\Gamma(\nu)} \int_{0}^{\infty} e^{-x} \left[x^{\nu-1}\, e^{-\vec{q}_{\perp}^{\,2}\, L_{\perp}^{2}\, x} \right] dx$$

$$\sim \frac{1}{\Gamma(\nu)} \sum_{i=1}^{M} w_{i} \left[x_{i}^{\nu-1}\, e^{-\vec{q}_{\perp}^{\,2}\, L_{\perp}^{2}\, x_{i}} \right] \quad , \tag{65}$$

where w_{i} and x_{i} are the Gauss-Laguerre weights and zeros. This allows the func-tion $\check{D}[\mathcal{K}]$ to be approximated by a sum of separable Gaussian $\check{D}[\mathcal{K}]$ as given in Eq. (57). A way to avoid retaining all of the $(M)^{n}$ terms that would appear in the nth convolution of $\check{D}[\mathcal{K}]$ is to approximate each nth order convolution $\check{D}[\mathcal{K}]$ by an appropriate new sum of Gaussians. A procedure for doing this is given in Appendix F.

Although we have utilized the eikonal approximation [Eq. (5)] to the full Green's function in the calculation thus far it is possible to give a completely general for-mulation for the cross section by using, in conjunction with the cumulant and con-volution expansions of the previous section, the operator representation for the full Green's function in an arbitrary external field developed by Fradkin[6] and

Milekhin.[10] In this method the full Green's function, starting from the Fourier transform of Eq. (5) is given by

$$\widetilde{G}(\vec{r}, \vec{p}) = - \left[(\vec{\nabla} - i\vec{p})^2 - k_o^2 \varepsilon(\vec{r}) \right]^{-1}$$

$$= i \int_0^\infty e^{is\left[(\vec{\nabla} - i\vec{p})^2 - k_o^2 \varepsilon(\vec{r}) \right]} ds$$

$$= i \int_0^\infty e^{is(-\vec{p}^2 + is\vec{\nabla}^2 + 2\vec{p}\cdot\vec{\nabla} - isk_o \varepsilon(\vec{r}))} ds \quad . \tag{66}$$

Milekhin has shown that the principal approximation that is necessary in deriving the eikonal limit corresponds to dropping the term [is ∇^2] in the exponent of Eq. (66). Operating with $e^{2s\vec{p}\cdot\vec{\nabla}}$ on $\varepsilon(\vec{r})$, shifts the argument from $\vec{r}$ to $\vec{r} + 2\vec{p}s$ and operator ordering leads to the eikonal form given in Eq. (5).

Calculation of the scattering cross section to include the effects of terms in the Green's function beyond the eikonal approximation is most straightforward if Fradkin's representation using functional derivatives is employed [Reference 6, Eq. (5.17)]. We shall, however, leave the calculation of the cross section including these higher order contributions to a future publication.

3. CROSS SECTION FOR GAUSSIAN FLUCTUATIONS

The behavior of the cross section can most easily be studied for the case where the correlation function $\langle \delta\varepsilon^2(\vec{r} - \vec{r}') \rangle$ is given by the factored Gaussian of Eq. (29). Looking first at the $n = 0$ (modified Born) term in Eq. (54) we have

$$\sigma^{[o]}_{\hat{K}_i, \hat{K}_f} = \frac{1}{4}\varepsilon^2 K^4 \pi^{1/2} L_\perp^2 L_\parallel e^{-(K_{iz} - K_{fz})^2 \frac{L_\parallel^2}{4}}$$

$$e^{-(\vec{K}_{i\perp} - \vec{K}_{f\perp})^2 \frac{L_\perp^2}{4}} \left[1 - \frac{e^{-(\beta_i + \beta_f)L}}{(\beta_i + \beta_f)L} \right] \quad . \tag{67}$$

10. Milekhin, G. A. (1963) The infrared asymptotic behavior of the Green's function in some problems of quantum field theory, Sov. Phys.—JETP 16, p. ...

For $L_{\parallel} \gg L_{\perp}$ this term will be small unless $k_{iz} \simeq k_{fz}$. The Born term will thus peak when $\chi_f \simeq \chi_i$ leading to essentially specular scattering. Multiscattering effects are contained in the term in brackets and appear as a path dependent attenuation for traversing the slab. For small L the exponent can be expanded and the bracketed term equals ~ 1, which is expected as multiscattering effects will not contribute unless the path length is longer than the mean free path between small angle scatterings ($\mathscr{L} \sim 1/2\alpha$). Due to the anisotropy of the medium, paths directed along the x axis $(\chi \sim \frac{\pi}{2})$ will be attenuated less per unit length than those directed more toward the Z axis $(\chi \sim 0)$ as can be seen from the expression for α_χ given in Eqs. (41) and (42). Recalling that β_i contains the geometric factor

$$\left[\frac{1}{\sin^2(\chi_i)} + \tan^2(\omega_i) \right]^{1/2} = T(\hat{K}_i) \tag{68}$$

the product

$$\beta_i L = 2\alpha_{\chi_i} \cdot L \cdot T(\hat{K}_i) \tag{69}$$

is seen to represent the path length from the front of the slab to the back of the slab along the ray $\hat{K}_i$ times the attenuation for that ray direction. Thus for shallow angle rays, in addition to the larger attenuation as a function of the polar angle χ, there will be an added reduction in the scattered power due simply to the longer path lengths that are required in traversing slab at shallow angles.

In order to determine the behavior of the $n > 1$ terms in Eq. (54) in an approximate way, we shall assume that $L_{\parallel} \gg L_{\perp}$ so that the scattering will be approximately spectral and set $\beta_i \sim \beta_f$. Taking $\beta_i L > 1$ we approximate $\gamma(n+1, 2\beta_i L)$ by $\Gamma(n+1) = n!$. The terms with $n > 1$ are then

$$\frac{1}{2^n L (\beta_i + \beta_f)} \sum_{n=1}^{\infty} \sum_{j=0}^{n} \frac{n!}{(n-j)! \, j!} \, D_i^{n-j}(\Delta \vec{r}) \, D_f^{j}(\Delta r) \sim \frac{D_i^n(\Delta \vec{r})}{[\beta_i \cdot 2L]} \ . \tag{70}$$

Using Eq. (57) for the nth order convolution, we then have very roughly an approximation for the behavior of $\sigma^{[n]}_{\hat{K}_i, \hat{K}_f}$ given by

$$\sigma^{[n]}_{\hat{K}_i, \hat{K}_f} \sim c \frac{e^{-(\Delta \vec{K}_\perp)^2 L_\perp^2/4(n+1)} \, e^{-\Delta K_z^2 L_\parallel^2/4(n+1)}}{(n+1)} \ . \tag{71}$$

The contributions to $\sigma_{\vec{K}_i \vec{K}_f}$ from the nth order multiscattering terms are thus reduced in amplitude by a factor $(n + 1)^{-1}$ and are broadened by a change in the effective half width from $1/L_{\parallel}$ to $\sqrt{n + 1}/L_{\parallel}$. This behavior is illustrated in the sketch of Figure 4.
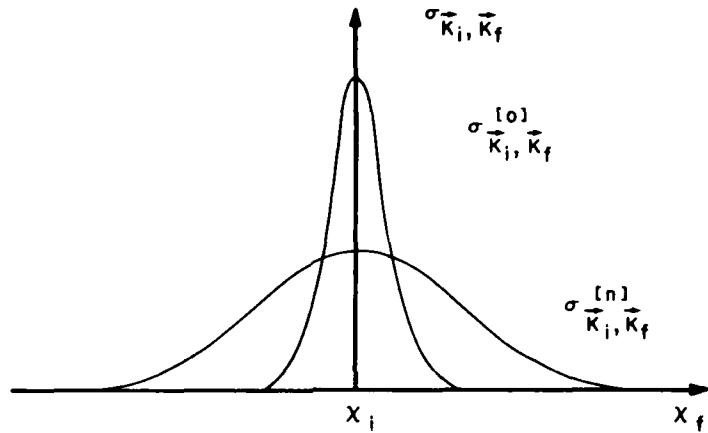

Figure 4. Sketch of Expected Behavior for o (Born) and nth Order Scattering Cross Section Contributions

Since we have indicated that each term $\sigma^{[n]}_{\vec{K}_i, \vec{K}_f}$ decreases in amplitude as $\frac{1}{(n + 1)}$ the series $\sum_{n=1}^{N} \sigma^{[n]}_{\vec{K}_i, \vec{K}_f}$ would appear to diverge as $\lim_{N \to \infty} \ln(N)$. However, if the approximation $\gamma(n +1, x) \simeq \Gamma(n)$ is not made, convergence of the series can be proved by using the integral representation for $\gamma(n + 1, x)$

$$\sum_{n=0}^{\infty} \frac{\gamma(n + 1, x)}{n! \, (n + 1)} = \sum_{n=0}^{\infty} \int_{o}^{x} \frac{e^{-t} t^n \, dt}{(n + 1)!}$$

$$= \int_{o}^{x} \frac{e^{-t}}{t} \sum_{n=0}^{\infty} \frac{t^{n+1}}{(n + 1)!} \, dt$$

$$= \int_0^x \frac{e^{-t}}{t} \left[\sum_{m=0}^{\infty} \frac{t^m}{m!} - 1 \right]$$

$$= - \int_0^x \frac{(e^{-t} - 1)}{t} \, dt$$

$$= -E_i(-x) + C + \ln(x)$$

$$= E_1(x) + C + \ln(x) \quad , \tag{72}$$

where $E_i(x)$, $E_1(x)$ are the exponential integral functions and C is Euler's constant.

For the case of an isotropic medium $L_{\parallel} = L_{\perp}$ and $\sigma_{\vec{K}_i, \vec{K}_f}$ will no longer depend on $\vec{K}_i$ and $\vec{K}_f$ individually, but only on their difference $\Delta\vec{K} = \vec{K}_f - \vec{K}_i$. The momentum transfer $\Delta\vec{K}$ may be written as

$$\Delta\vec{K}^2 = (\vec{K}_i - \vec{K}_f)^2 = K^2(2 - 2\cos(\theta)) = K^2 \left(2 \sin\left(\frac{\theta}{2}\right) \right)^2 \quad , \tag{73}$$

where θ, the angle between $\vec{K}_i$ and $\vec{K}_f$, is defined by

$$\cos(\theta) = \hat{K}_i \cdot \hat{K}_f = \sin(\chi_i) \sin(\chi_f) \cos(\phi_i - \phi_f) + \cos(\chi_i) \cos(\chi_f) \tag{74}$$

where the angles χ, ϕ are defined in Figure 2. If we take $\phi_i = 0$, $\phi_f = \pi$ then $\theta = \chi_i + \chi_f$, and we thus expect

$$\sigma_{\vec{K}_i, \vec{K}_f}^{[n]} \sim \frac{e^{-\Delta K^2 \ell^2 / 4(n+1)}}{(n + 1)} \tag{75}$$

to decrease (for $\chi_i (> 0)$ fixed) as χ_f increases, as sketched in Figure 5 for the case L = 0. For a slab of small but finite thickness, the path length in the $\chi_f = 0$ direction becomes infinite, cutting off scattering in this direction, whereas for a thick slab the scattering will be reduced for all $\chi_f > 0$ as well. This behavior is sketched in Figure 5 where $\chi_f < 0$ means $\chi_f = |\chi_f|$, $\phi_f = 0$, that is, scattering into the forward direction.
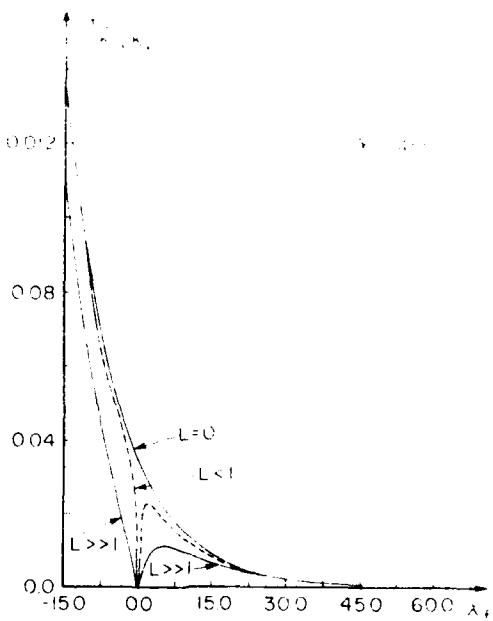
Figure 5. Sketch of Expected Behavior of
Scattering Cross Section as a Function of κ_f,
and Various Choices of Slab Thickness L.

4. NUMERICAL RESULTS FOR THE MULTISCATTER CROSS SECTION FOR $\Phi = \Phi_G$

In Figures 6a through 11e we have plotted for the case of a Gaussian correlation function: the total cross section [Eq. (54)]

$$\sigma^{[n]}_{\vec{K}_i, \vec{K}_f} = \sum_{n=0}^{10} \sigma_{\vec{K}_i, \vec{K}_f} \quad ,$$

the modified Born cross section $\sigma^{[o]}_{\vec{K}_i, \vec{K}_f}$, and the multiscattering contribution

$$\sigma^M_{\vec{K}_i, \vec{K}_f} = \sum_{n=1}^{10} \sigma^{[n]}_{\vec{K}_i, \vec{K}_f}$$

as functions of χ_f for χ_i fixed (with $\phi_i = 0$, $\phi_f = \pi$, $\epsilon = 0.03$) The starred curve represents $\sigma^{[o]}_{\vec{K}_i, \vec{K}_f}$, the highest solid curve $\sigma_{\vec{K}_i, \vec{K}_f}$, and their difference is the remaining solid curve $\sigma^{M}_{\vec{K}_i, \vec{K}_f}$.

In Figures 6a through 6e we have plotted the cross section for the case of a thin slab (L = 1.) for which the total cross section essentially equals the Born cross section with multiscattering effects being mainly due to the attenuation of the random medium, as discussed as the beginning of Section 3. The anisotropy aspect ratio $\eta = \dfrac{L_\parallel}{L_\perp}$ varys from $\eta = 2$, in Figure 6a which appears almost iso-tropic, to $\eta = 32$ in Figure 6e. The expected behavior for $\eta = 1$ was discussed previously and sketched in Figure 5. For $\eta = 2$ the situation is seen to be quite similar. There is a small contribution due to $\sigma^{M}_{\vec{K}_i, \vec{K}_f}$ which falls off exponentially as χ_f increases. As η is increased to $\eta = 4$ the Born term develops two peaks. From Eq. (67) we see that the Born term will be given by a product of Gaussians (for the case L = 1 the attenuation factor is ≈ 1)

$$\sigma^{[o]}_{\vec{K}_i, \vec{K}_f} \simeq \frac{1}{4}\, \epsilon^2\, K^4\, \pi^{1/2}\, L_\perp^2\, L_\parallel\, e^{-\Delta K_z^2 L_\perp^2 \eta^2 /4}\, e^{-\Delta \vec{K}_\perp^2 L_\perp^2 /4}$$

with

$$\Delta K_z^2 = K^2 \left(\cos(\chi_f) - \cos(\chi_i)\right)^2$$

$$\Delta \vec{K}_\perp^2 = K^2 \left(\sin(\chi_f) + \sin(\chi_i)\right)^2$$

and

$$\cos(\chi_i) = \sin(\chi_i) = \frac{\sqrt{2}}{2}\ , \quad \chi_i = 45^{\circ}\ .$$

The Gaussian with argument proportional to $\Delta \vec{K}_\perp^2$ peaks at $\chi_f = 0$, while that with argument proportional to $\Delta K_z^2 \eta^2$ peaks at $\chi_f = \chi_i$. Their product will thus have a minimum somewhere between $\chi_f = 0$ and $\chi_f = \chi_i$ (unless $\eta = 1$) and this is reflected by the dip seen in Figure 6b at $\chi_f \sim 11^{\circ}$. As η is increased to $\eta = 8$ in Figure 6c, the term $\exp(-L_\perp^2 K_z^2 \eta^2/4)$ dominates and the scattering cross section becomes peaked around $\chi_f = \chi_i$.

Increasing η to $\eta = 16$ and $\eta = 32$ as shown in Figures 6d and 6e results in narrower peaks with larger maxima. The integrated cross section remains

31

approximately constant however, since the correlation function is normalized, that is,

$$\sqrt{\pi}\ L_{\parallel} \int_{-\infty}^{\infty} dK_z\ e^{-K_z^2 L_{\parallel}^2/4} = 1$$

and for very narrow peaks

$$dK_z = d[K \cos(\chi_f)] = -[\sin(\chi_f) K]\ d\chi_f \simeq const \cdot d\chi_f$$

as $\sin(\chi_f)$ is essentially constant over the main contribution to the integrated cross section.

In Figures 7a through 7e all parameters remain the same as in Figures 6a through 6e except that the random medium is now taken to be a thick rather than a thin slab (L = 10000 vs. L = 1). Multiscattering and path length attenuation will thus play a larger role. Comparing Figures 7c through 7e with Figures 6c through 6e, it can be seen that the change in the modified Born contribution $\sigma^{[o]}_{\vec{K}_i, \vec{K}_f}$ is entirely due to the attenuation factor $\left[1 - e^{-(\beta_i + \beta_f)L}\right] / \left[(\beta_i + \beta_f)L\right]$, which around the peak $\chi_f = 45^o$, equals $\simeq 0.0046$. The multiscattering contribution for the thick slab case is broader than the Born term as discussed previously and is of comparable magnitude. For Figures 7a and 7b the implication of a thicker slab for the Born term is that the attenuation factor, instead of being ≈ 1 for all angles will now be angle dependent, being much smaller at shallow angles due to the increased path length in the medium (as well as the effect of α_χ being somewhat larger for shallow angles). This has the effect of suppressing the small angle peaks of Figures 6a and 6b resulting in the broadened and reduced peaks of Figures 7a and 7b.

The multiscatter contributions $\sigma^{M}_{\vec{K}_i, \vec{K}_f}$ in Figures 7a and 7b are seen to be broader but roughly similar in shape to the modified Born terms. They are, however, of greater magnitude being more than twice the Born cross section for $\eta = 2$.

In Figures 8a through 8e χ_i has been reduced from $\chi_i = 45^o$ to $\chi_i = 15^o$, all other parameters being the same as those in Figures 7a through 7e. The main difference in the plots for large η, $\eta = 8$, 16, 32 is that the peaks for $\chi_i = 15^o$ are much broader than those for $\chi_i = 45^o$ about their respective maxima, as well as being larger (by $\sim 10^2$). If we look at the dominant factor in the Born term $b_i(K_{fz}) = e^{-(K_{iz} - K_{fz})^2 L_{\parallel}^2/4}$, this would yield a curve with the same half width about

any value for K_{iz} if plotted as a function of K_{fz}. As Figures 6a through 6e have been plotted as a function of χ_f, a plot of

$$b_i [K \cos(\chi_f)] \text{ vs } \chi_f$$

will be broader for curves peaked around smaller χ_i since

$$|dK_{fz}| = \sin(\chi_f) K \cdot d\chi_f$$

that is, equal increments of $d\chi_f$ yield a smaller change in K_{fz} for small $\chi_f (\chi_f \sim 0^0)$ than they do for large $\chi_f (\chi_f \sim 90^0)$. The fact that the values of $\sigma^{[o]}_{K_i, K_f}$ at $\chi_f = 15^0$ in Figures 8a through 8e are larger than in Figures 7a through 7e is due to the second factor in the Born term [Eq. (67)]

$$e^{-\Delta K^2 1_z^2/4} = e^{-(\sin \chi_i + \sin \chi_f)^2 K^2 1_z^2/4}$$

Thus

$$e^{-(2 \times .707)^2 K^2 1_z^2/4} \geq 4.9 \times 10^{-4} \quad \text{for} \quad \chi_i = 45^0$$

vs

$$e^{-(2 \times .2.59)^2 K^2 1_z^2/4} \geq 3.6 \times 10^{-1} \quad \text{for} \quad \chi_i = 15^0 \quad,$$

along with a factor of ~ 0.125 due to the larger attenuation for the shallow angle paths in Figures 8e through 8e, lead to the observed difference in these peak maxima which amounts to a factor of $\sim 10^4$ with respect to the peak maxima of Figures 7e through 7e.

For $\chi_i = 45^0$ the peak multiscattering contribution with respect to the Born contribution runs from about $\frac{\sigma^M}{\sigma^{[o]}} \simeq 0.5$ for $\eta = 32$ to $\frac{\sigma^M}{\sigma^{[o]}} \simeq 2.3$ for $\eta = 2$, while for $\chi_i = 15^0$ the ratio runs from 0.5 to 1.

In Figures 9a through 9e the cross section for $\eta = 4$, $\chi_i = 45^0$, $K = 2\pi/1.6$ is plotted for $L = 1., 10, 100, 1000$, and 10000. The double peak in Figure 9a was discussed previously for Figure 6b (Figure 6b = Figure 9a). As L is increased to 10 the low angle peak in the Born term is suppressed while the peak around χ_i is lowered slightly. Since the only L dependence in the Born term [Eq. (67)] is in the attenuation factor, the low angle suppression is due to the increase in l'_f at low angles (for $L = 1$ the attenuation factor is ~ 1). As L is increased beyond 10, the

attenuation factor behaves roughly as $1/(\beta_i + \beta_f) L$, which is reflected in the behavior of $\sigma^{[o]}_{\vec{K}_i, \vec{K}_f}$ in Figures 9c through 9e.

In Figures 10a through 10e and 11a through 11e we have plotted the multiscatter cross sections for increasing values of χ_i, $\chi_i = 5^o$, 15°, 45°, 75°, 85°; for $K = 2\pi/1.6$ ($\eta = 4$, $L = 10000$) in Figures 10a through 10e, and for $K = 2\pi/0.8$ ($\eta = 4$, $L = 10000$) in Figures 11a through 11e. In Figures 10a and 10b the peak cross sections are roughly comparable and $\sigma^M_{\vec{K}_i, \vec{K}_f}$ is roughly equal to $\sigma^{[o]}_{\vec{K}_i, \vec{K}_f}$.

For $\chi_i = 45^o$, 75°, and 85° (Figures 10c through 10e) $\sigma^M_{\vec{K}_i, \vec{K}_f}$ is still roughly comparable to $\sigma^{[o]}_{\vec{K}_i, \vec{K}_f}$ however the peak cross sections drop rapidly for $\chi_i = 45^o$ and beyond, due to the factor $e^{-\Delta K_\perp^2 L_\perp^2/4}$, which becomes exponentially smaller around the peak at χ_i as $\chi_i \rightarrow 90^o$. Thus a doubling of K from $K = 2\pi/1.6$ to $K = 2\pi/0.8$ means that the cross section around the peak at $\chi_f = \chi_i$ is given roughly by $\sigma(K = 2\pi/0.8) \sim [\sigma(K = 2\pi/1.6)]^4$, which accounts for the orders of magnitude difference between Figures 10c through 10e and the comparable Figures 11c through 11e. If instead of the Gaussian correlation function we had employed the Kolmogoroff spectrum [Eq. (30) with $\mu = 5/6$], this would lead to a corresponding change in the cross section around the peak of roughly

$$\sigma \left(K = \frac{2\pi}{.8} \right) \sim \left[\sigma \left(K = \frac{2\pi}{1.6} \right) \right] \Big/ 16 \quad ,$$

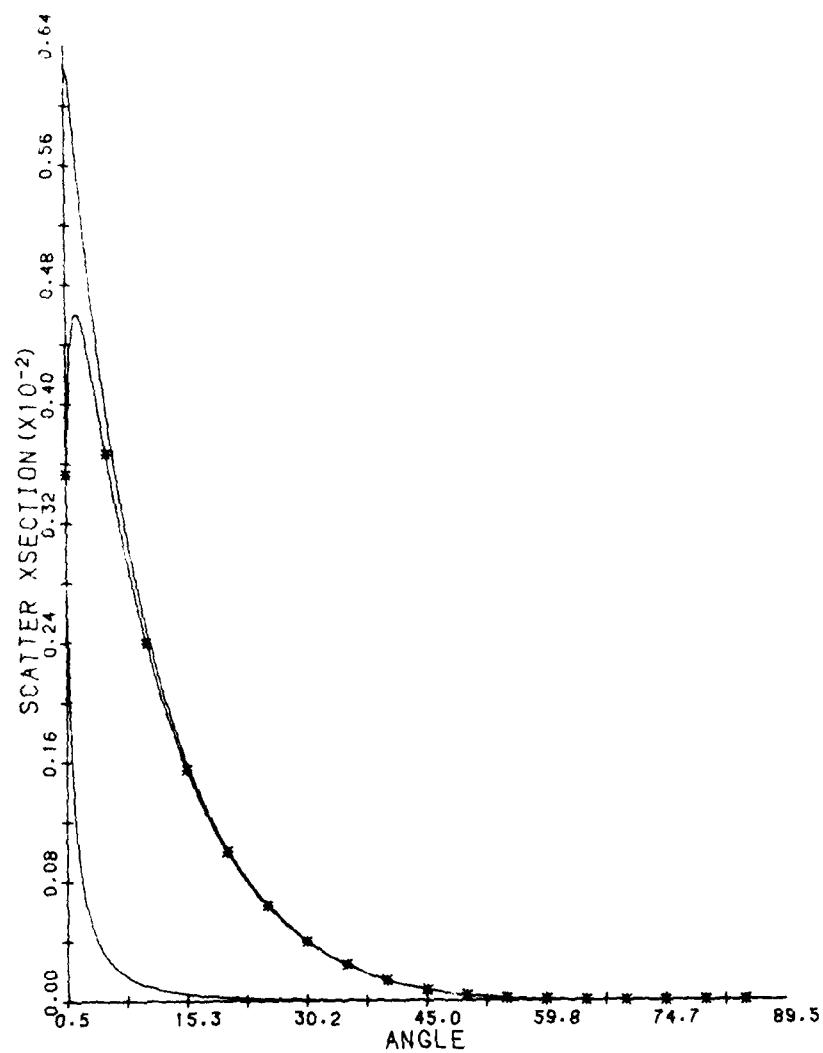that is, one to two orders of magnitude vs. ~ 20 orders of magnitude for the Gaussian.

Figure 6a. Plot of Modified Born, Multiscattering, and Total Cross Section as a Function of χ_f for: $\chi_i = 45^\circ$, $\eta = 2$, $L = 1$, $\lambda = 1.6$
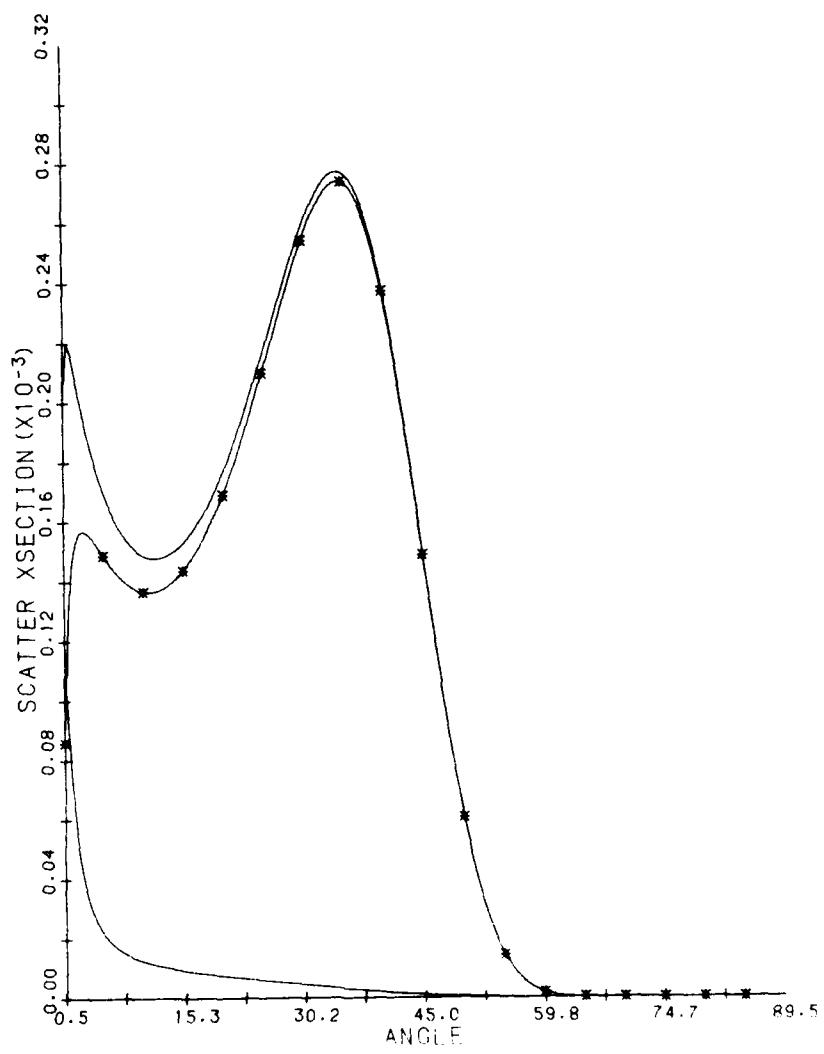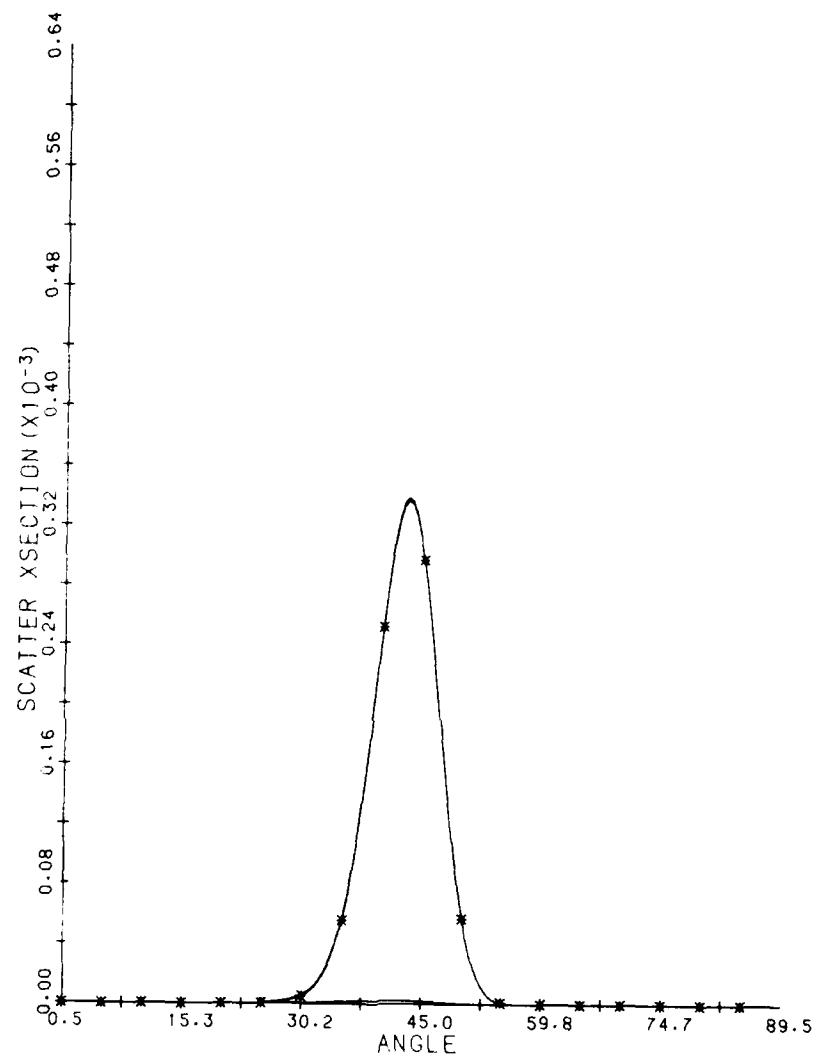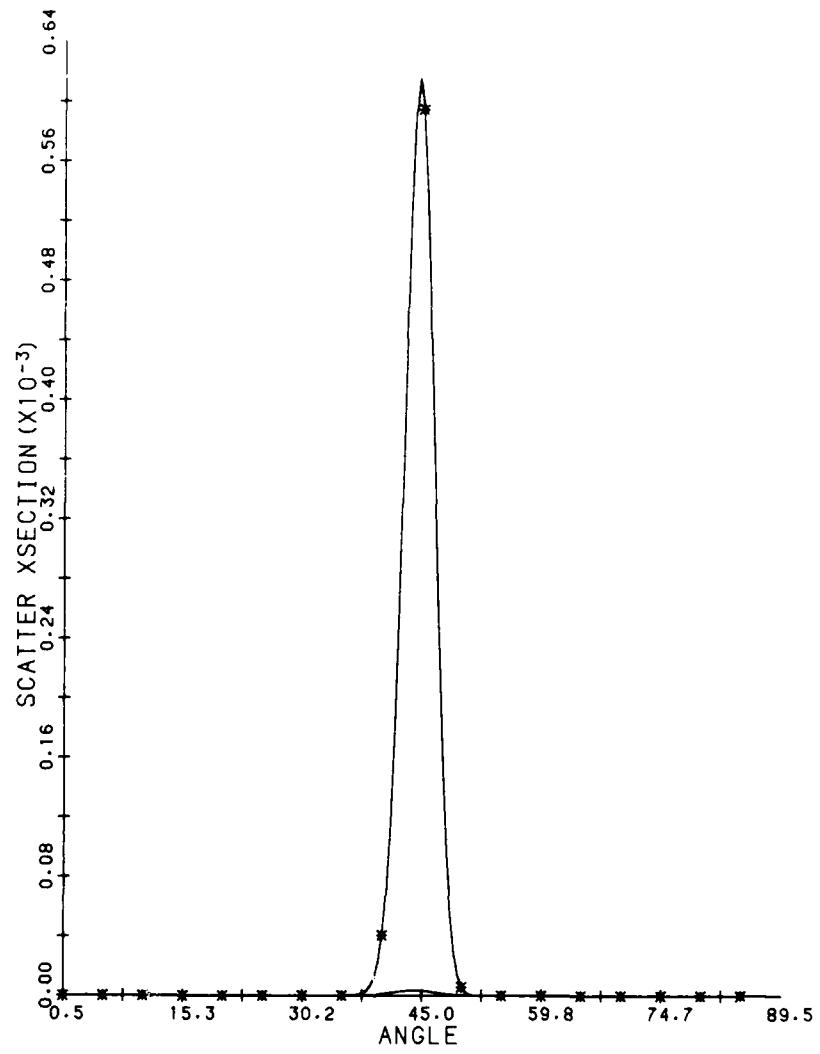
Figure 6b. Plot of Modified Born, Multiscattering, and Total Cross Section as a Function of χ_f for: $\chi_i = 45^0$, $\eta = 4$, $L = 1$, $\lambda = 1$.

Figure 6c. Plot of Modified Born, Multiscattering, and Total Cross Section as a Function of χ_f for: $\chi_i = 45^\circ$, $\eta = 3$, L = 1, $\lambda = 1.4$
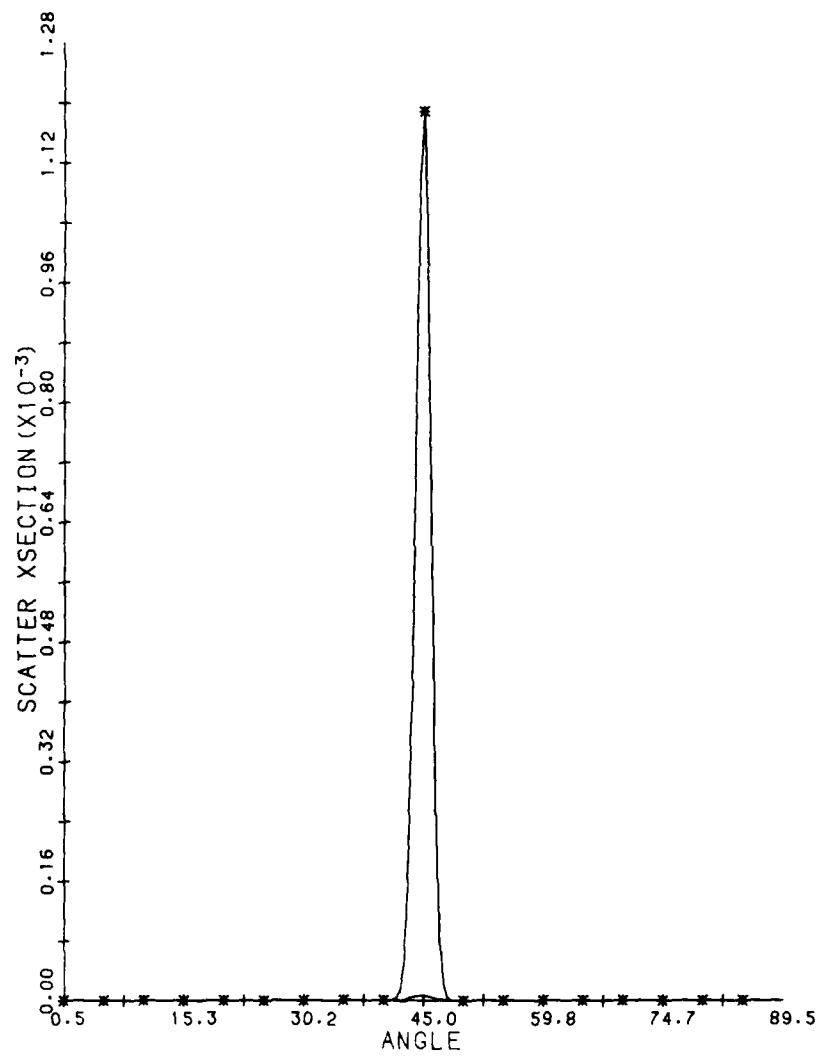
Figure 6d. Plot of Modified Born, Multiscattering, and Total Cross Section as a Function of χ_f for: $\chi_i = 45°$, $\eta = 16$, $L = 1$, $\lambda = 1.6$

38

Figure 6c. Plot of Modified Born, Multiscattering, and Total Cross Section as a Function of χ_f for: $\chi_i = 45°$, $n = 32$, $L = 1$, $\lambda = 1.6$
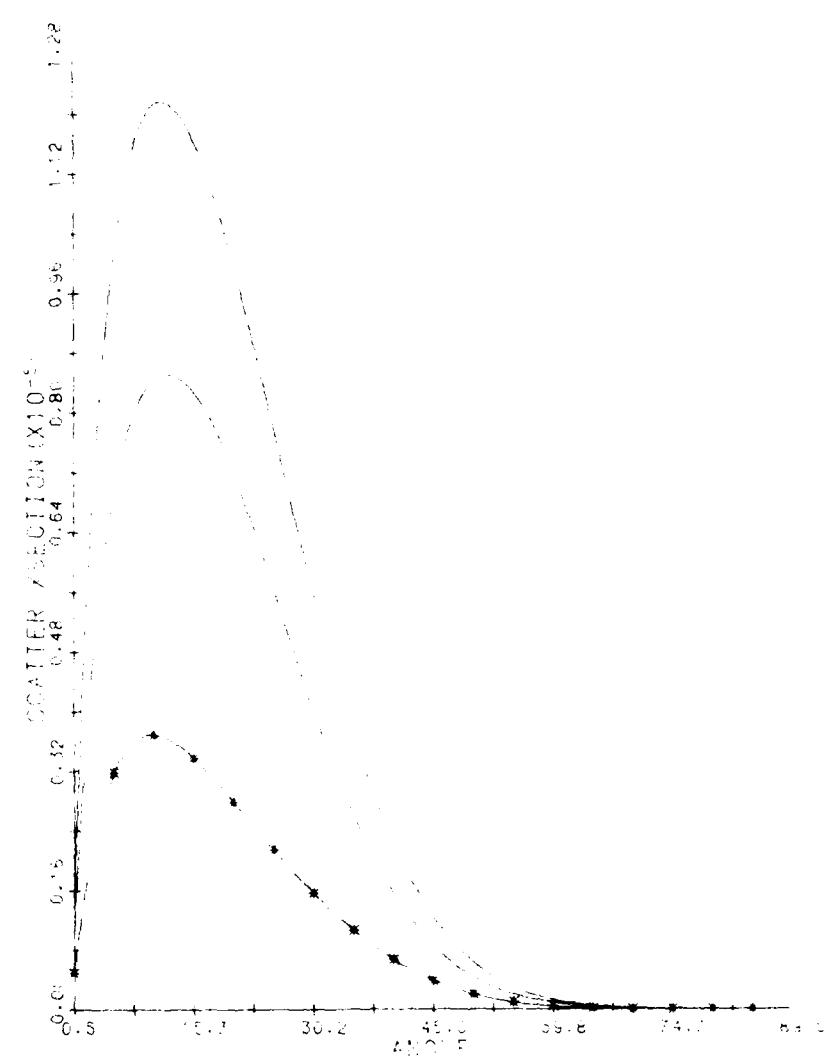
Figure 7a. Plot of Modified Born, Multiscattering, and total Cross Section as a Function of φ for: N_s = 4.0, n = 2.0, L = 10 mm, λ = 1.0
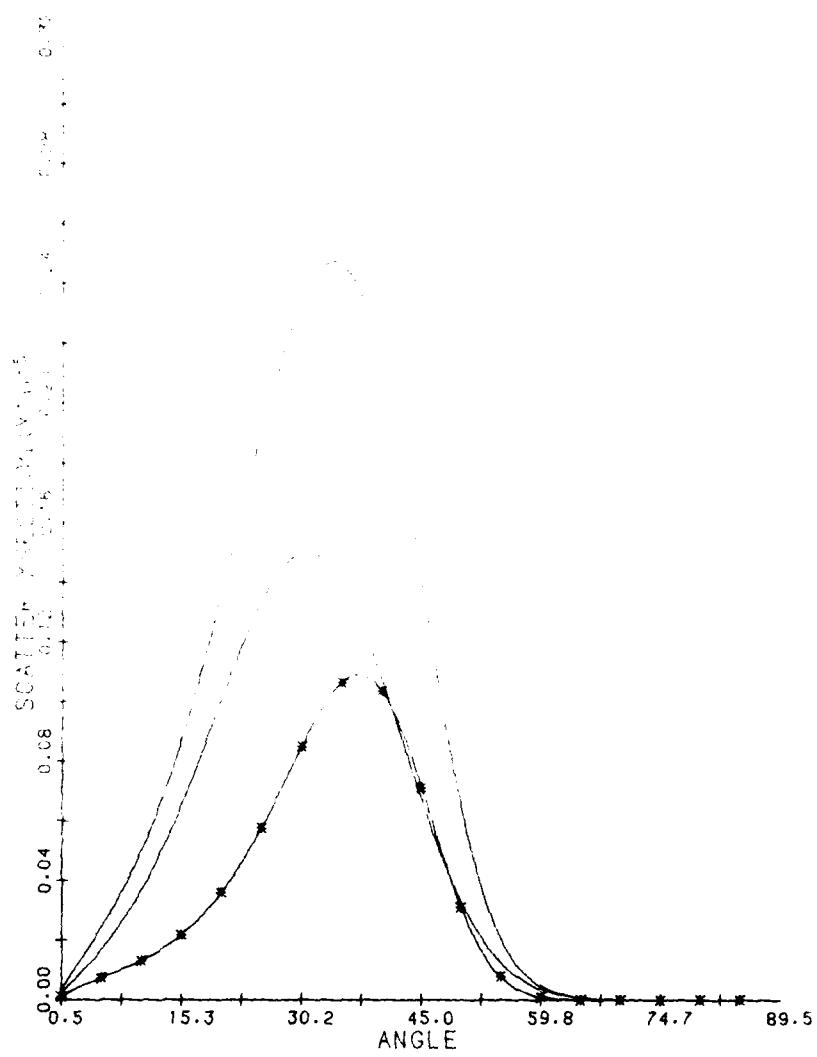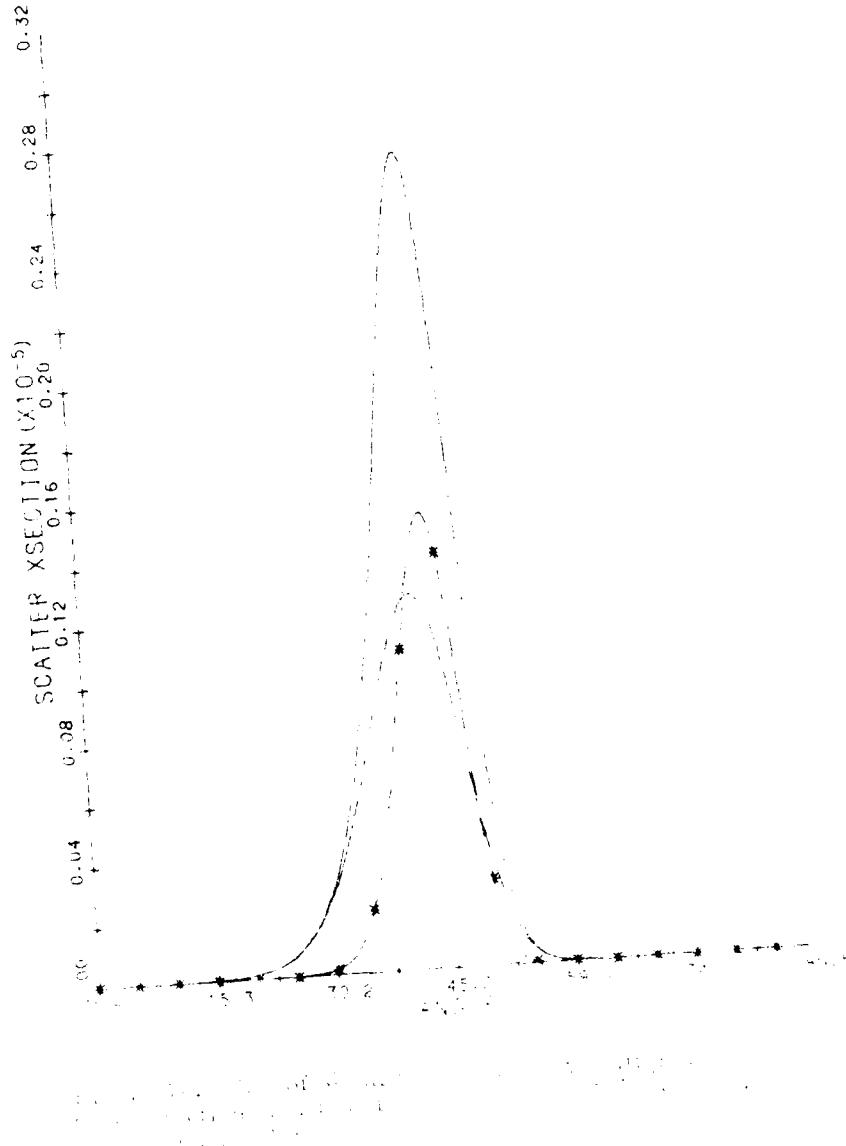
Figure 7b. Plot of Modified Born, Multiscattering, and Total Cross Section as a Function of x_f for: $x_i = 45^\circ$, $\eta = 4$, $L = 100m$, $\lambda = 1.0$

Figure 7d. Plot of Modified Born, Multiscattering, and Total Cross Section as a Function of χ_f for: $\chi_i = 45^o$, $\eta = 16$, L = 10000, $\lambda = 1.6$
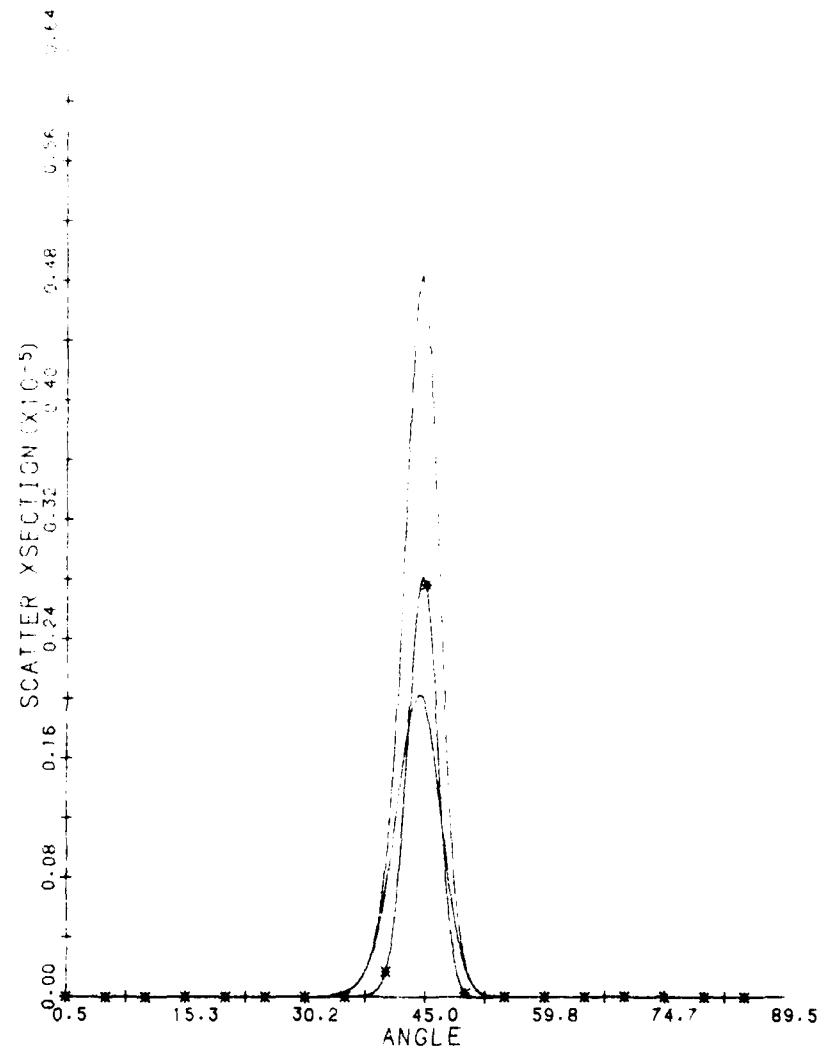
Figure 7e.   Plot of Modified Born, Multiscattering, and Total
Cross Section as a Function of χ_f for: $\chi_i = 45°$, $\eta = 32$,
$L = 10000$, $\lambda = 1.6$

Figure 8a. Plot of Modified Born, Multiscattering, and Total
Cross Section as a Function of ψ_f for: $\psi_i = 15^\circ$, $\eta = 2$,
$L = 100 m$, $\lambda = 1.6$

Figure 8b. Plot of Modified Born, Multiscattering, and Total
Cross Section as a Function of χ_f for: $\chi_i = 15^\circ$, $\eta = 4$,
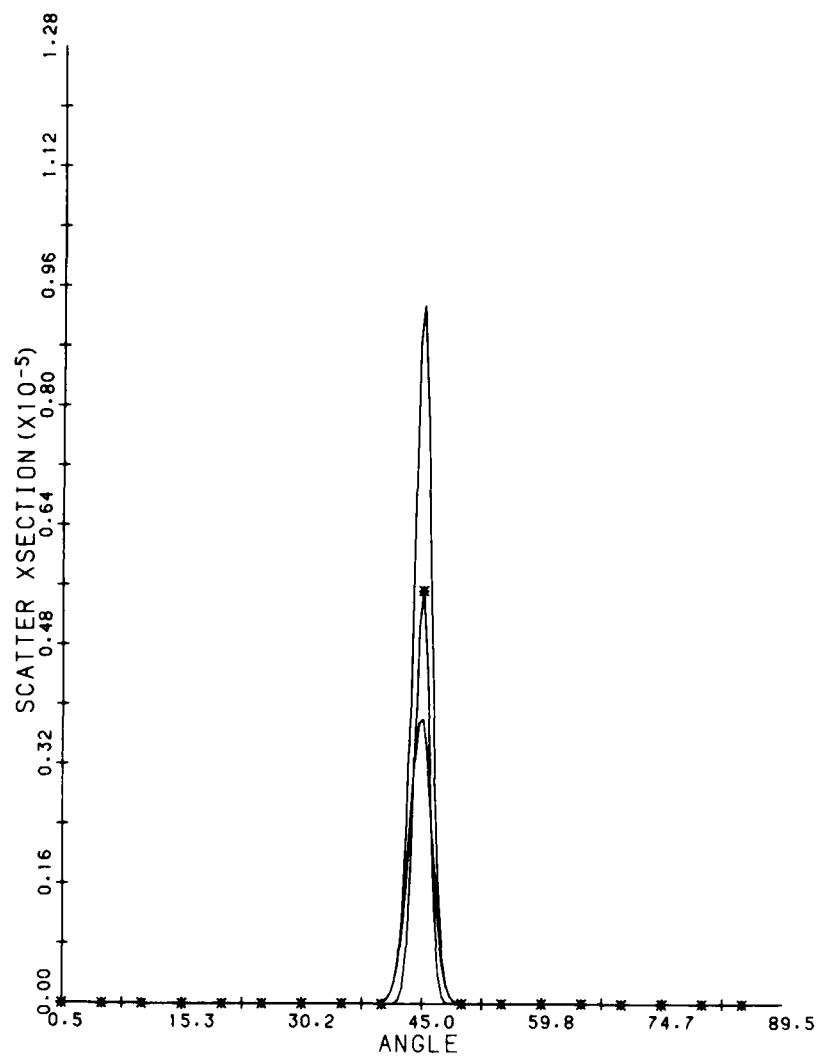$L = 10000$, $\lambda = 1.6$

SCATTER XSECTION (X10^{-3})

0.32 0.28 0.24 0.20 0.16 0.12 0.08 0.04 0.00

0.5   15.3   30.2   45.0   59.8   74.7   89.5

ANGLE

Figure 8c. Plot of Modified Born, Multiscattering, and Total Cross Section as a Function of χ_f for: $\chi_i = 15^\circ$, $\eta = 8$, $L = 10000$, $\lambda = 1.6$
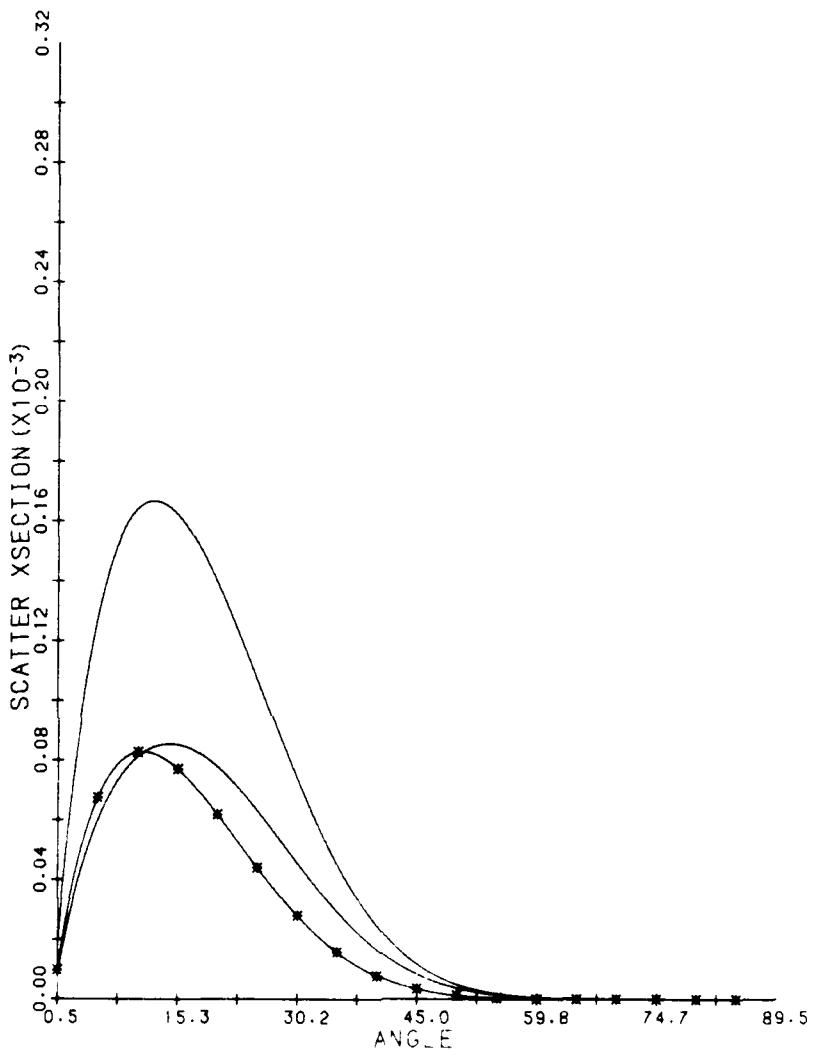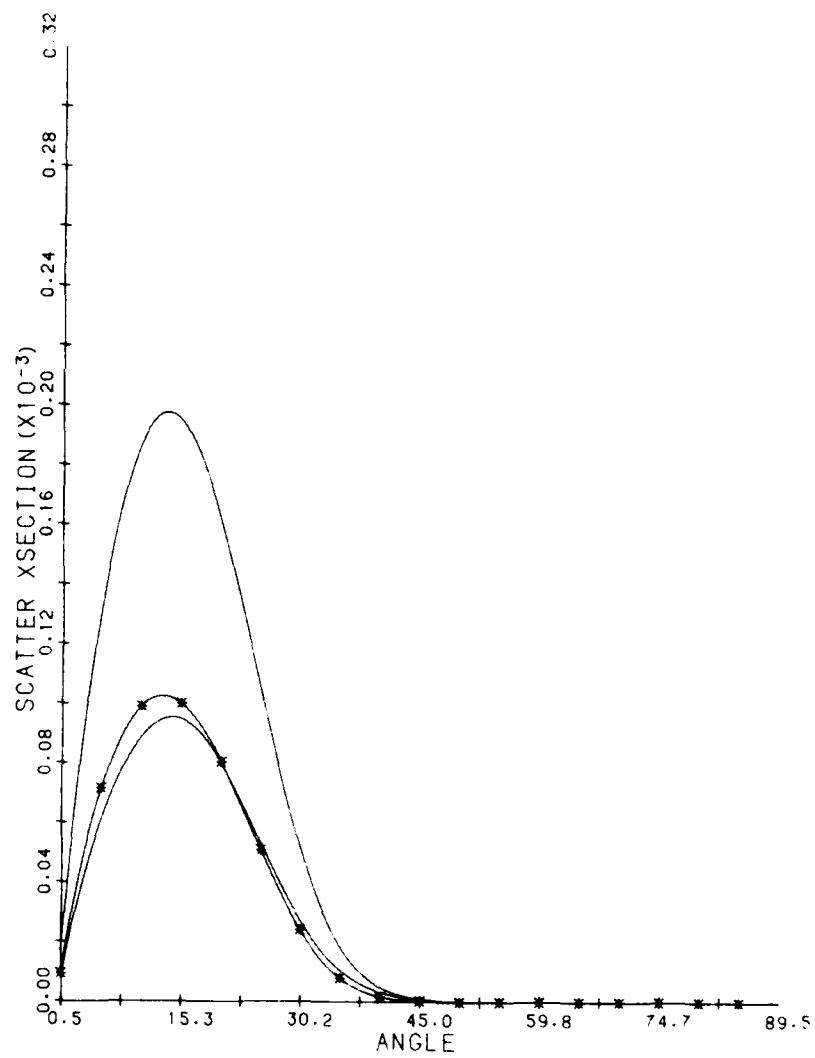
47

Figure 8d. Plot of Modified Born, Multiscattering, and Total Cross Section as a Function of χ_f for: $\chi_i = 15°$, $\eta = 16$, $L = 10000$, $\lambda = 1.6$

Figure 8e.   Plot of Modified Born, Multiscattering, and Total
Cross Section as a Function of χ_f for: $\chi_i = 15°$, $\eta = 32$,
L = 10000, $\lambda = 1.6$

49

Figure 9a.   Plot of Modified Born, Multiscattering, and Total
Cross Section as a Function of χ_f for: $\chi_i = 15^\circ$, $\eta = 4$, $L = 1$,
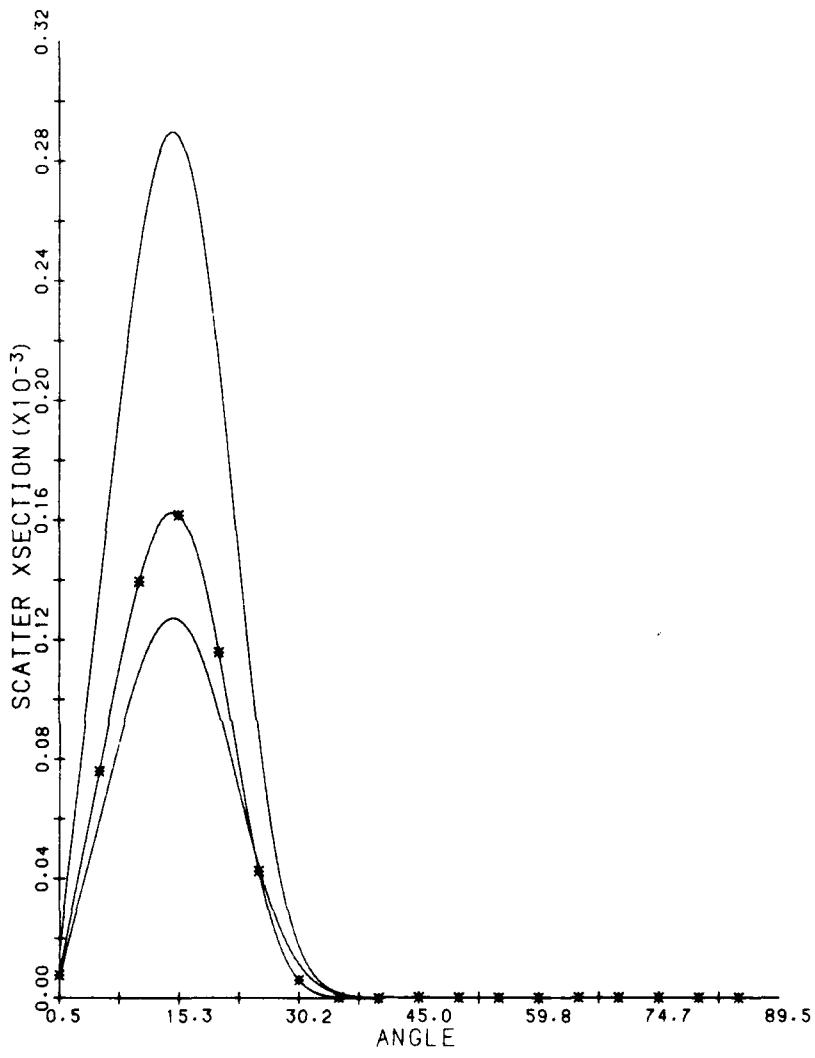$\lambda = 1.6$

Figure 9b. Plot of Modified Born, Multiscattering, and Total Cross Section as a Function of χ_f for: $\chi_i = 45^o$, $n = 4$, $L = 10$, $\lambda = 1.6$

Figure 9c. Plot of Modified Born, Multiscattering, and Total Cross Section as a Function of χ_f for: $\chi_i = 45°$, $\eta = 4$, L = 100, $\lambda = 1.6$

Figure 9d. Plot of Modified Born, Multiscattering, and Total Cross Section as a Function of χ_f for: $\chi_i = 45^o$, $\eta = 4$, $L = 1000$, $\lambda = 1.6$

53

Figure 10b.   Plot of Modified Born, Multiscattering, and Total Cross Section as a Function of χ_f for: $\chi_i = 15^O$, $\eta = 4$, $L = 10000$, $\lambda = 1.6$
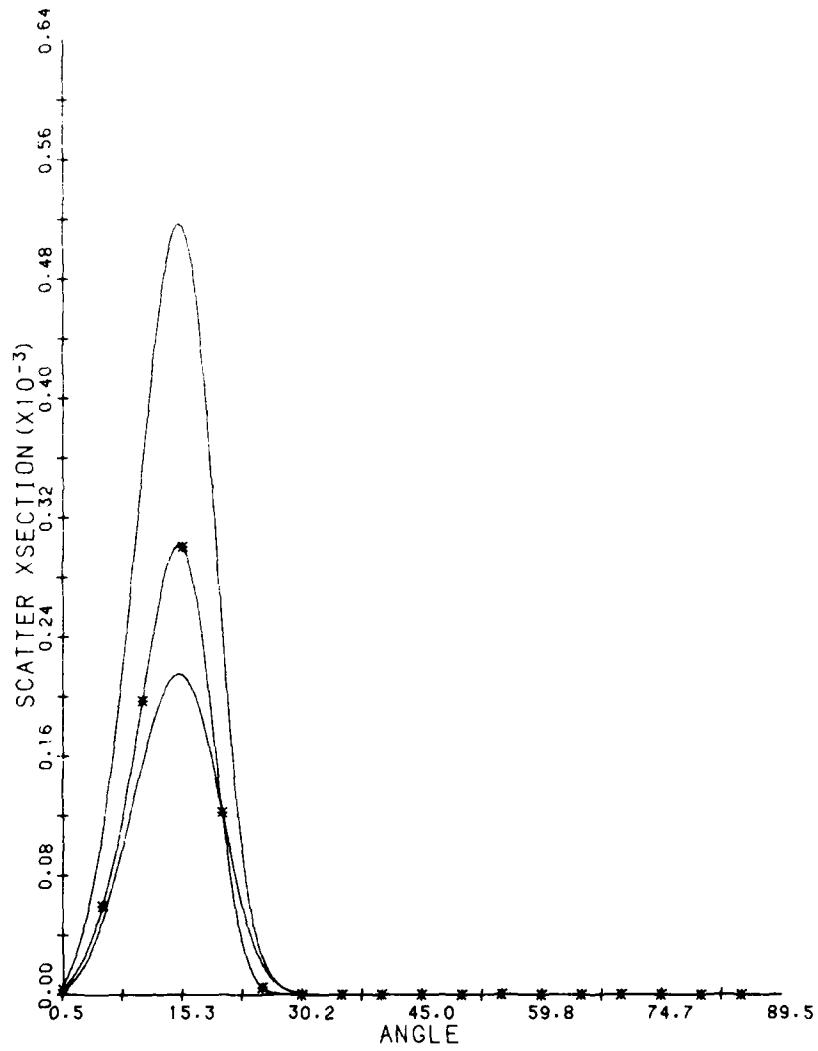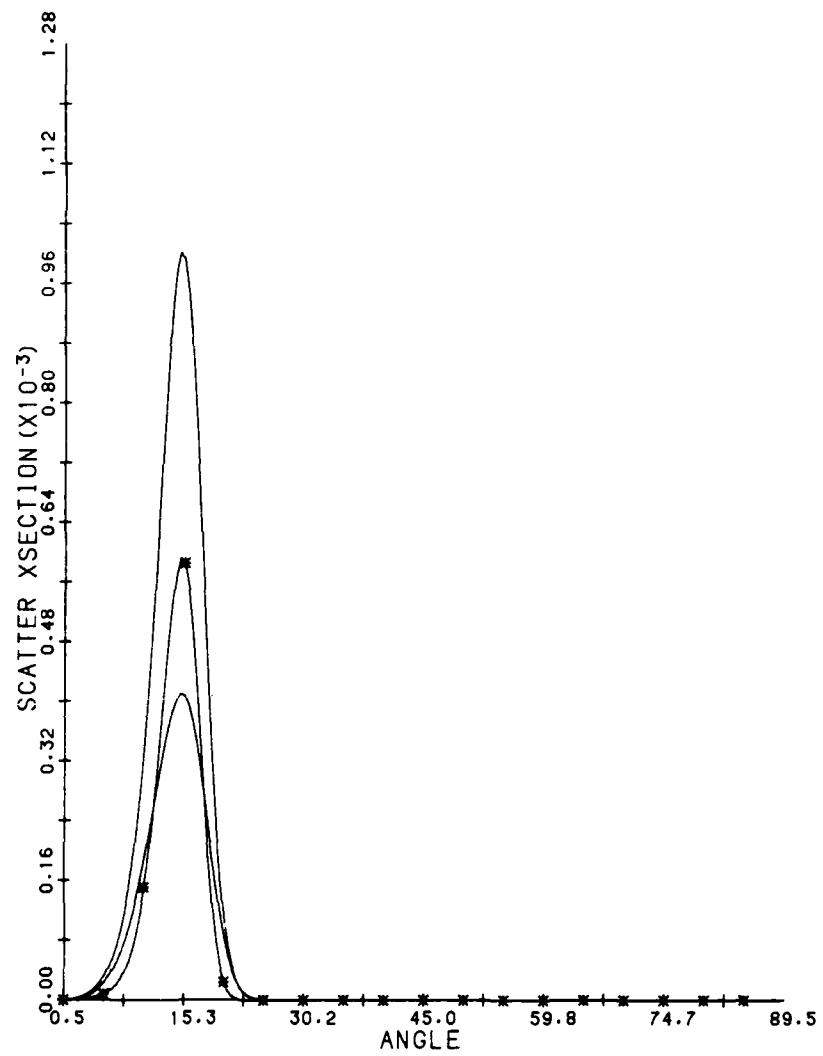
56
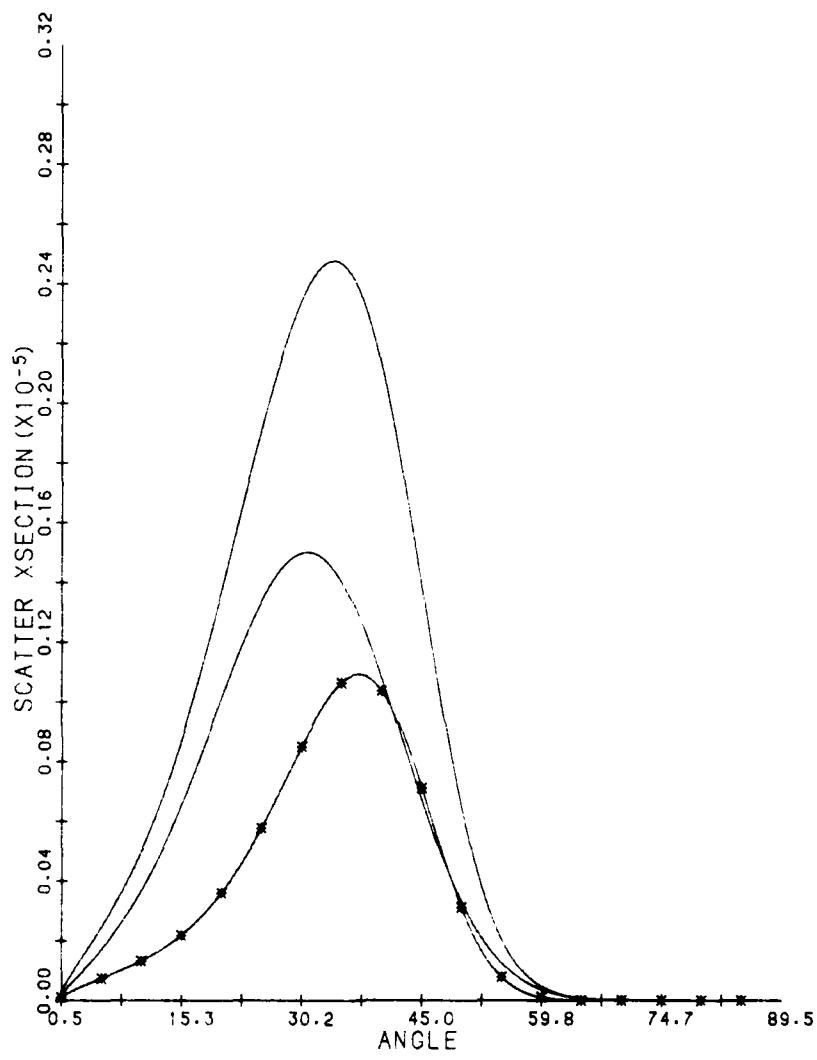
Figure 10c. Plot of Modified Born, Multiscattering, and Total Cross Section as a Function of χ_f for: $\chi_i = 45^o$, $\eta = 4$, $L = 10000$, $\lambda = 1.6$
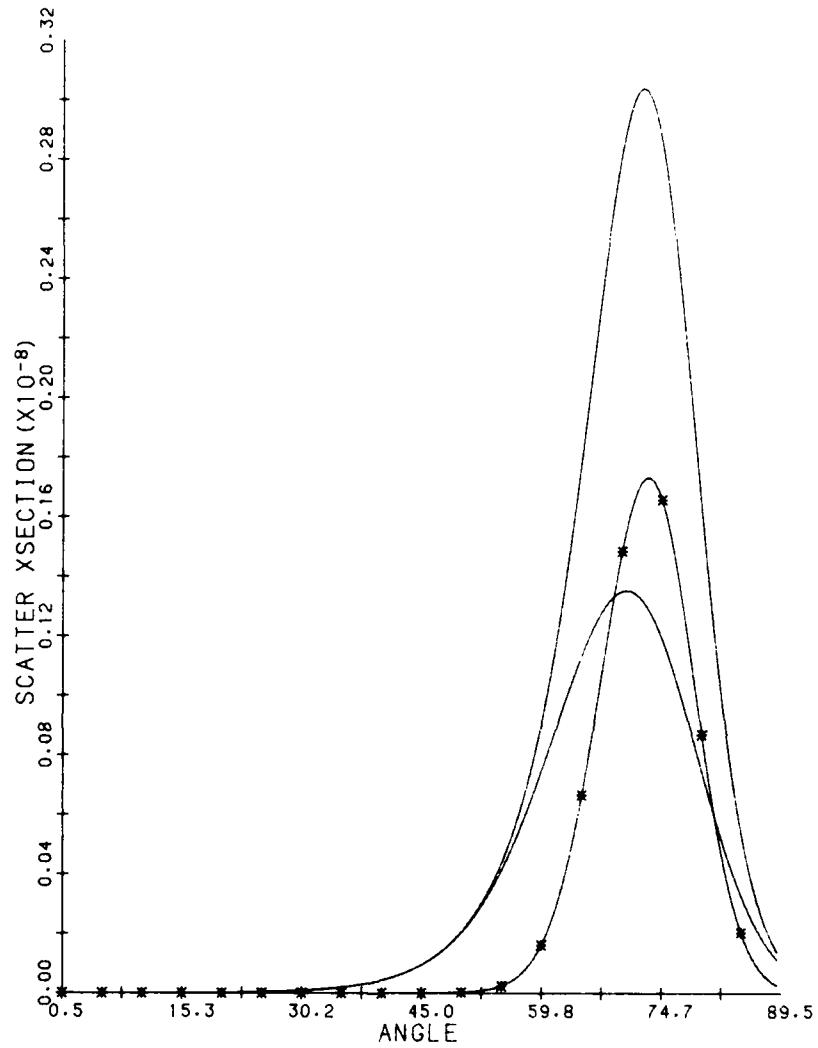
Figure 10d. Plot of Modified Born, Multiscattering, and Total Cross Section as a Function of χ_f for: $\chi_i = 75^O$, $\eta = 4$, $L = 10000$, $\lambda = 1.6$
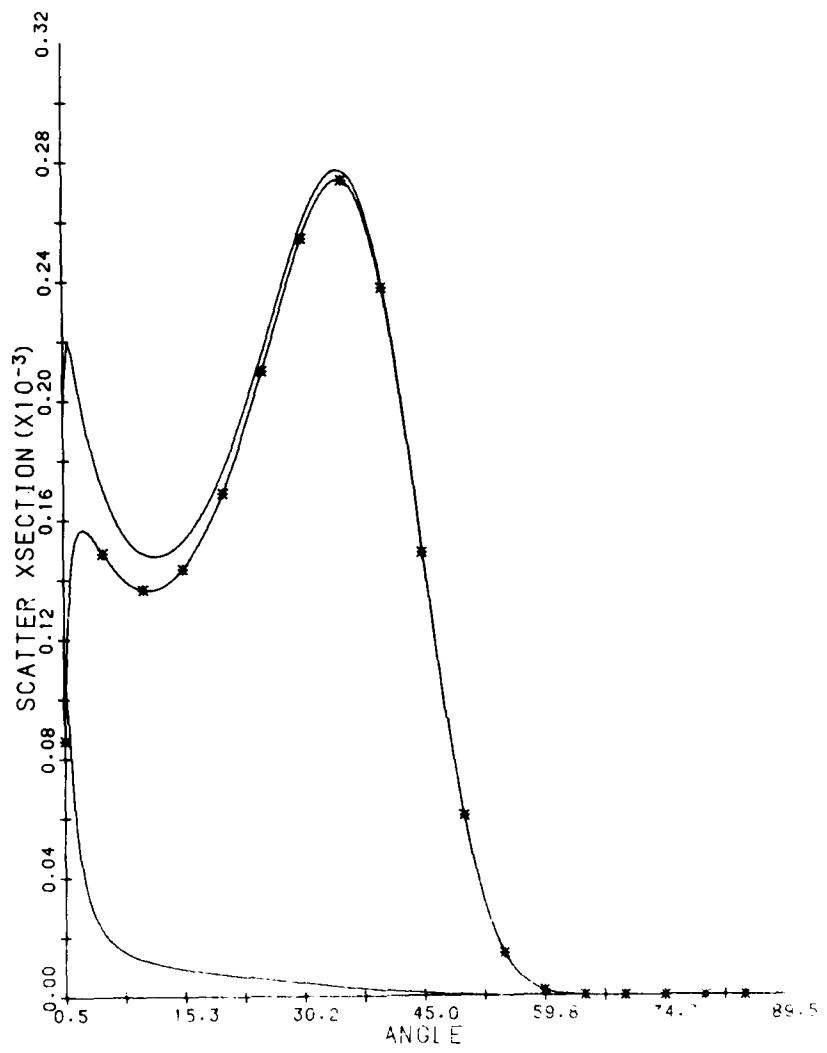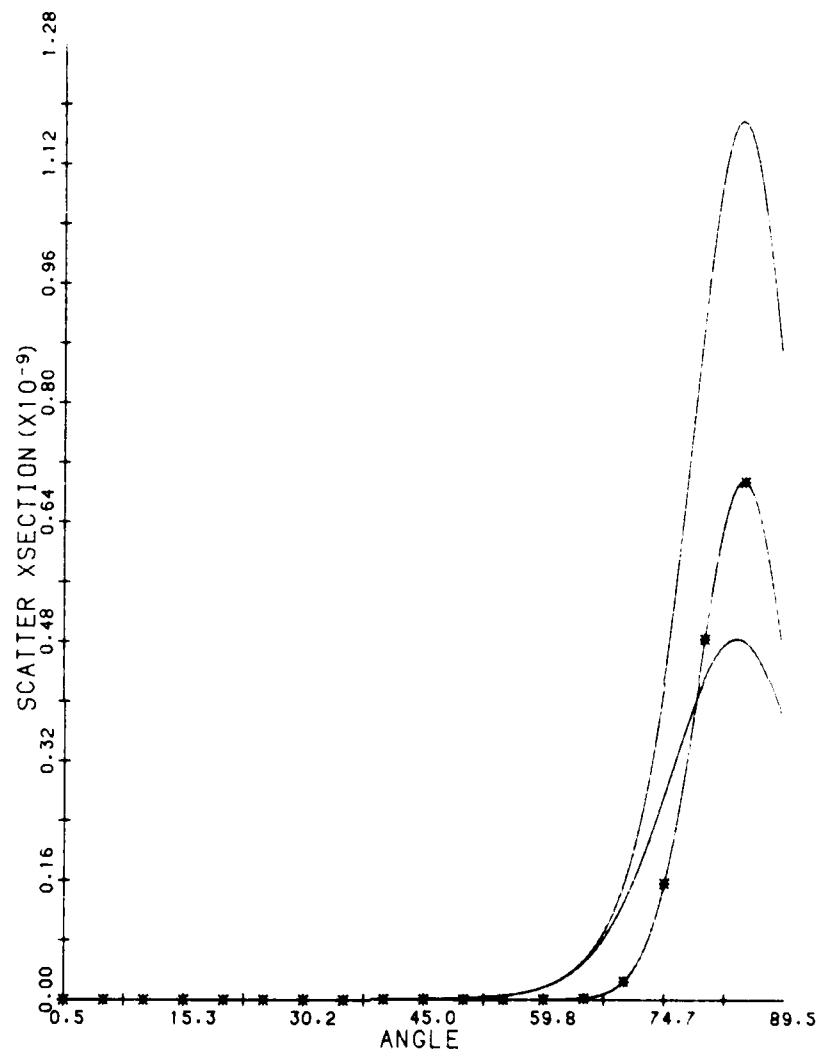
Figure 10e. Plot of Modified Born, Multiscattering, and Total
Cross Section as a Function of χ_f for: $\chi_i = 85^{\circ}$, $\eta = 4$,
$L = 10000$, $\lambda = 1.6$
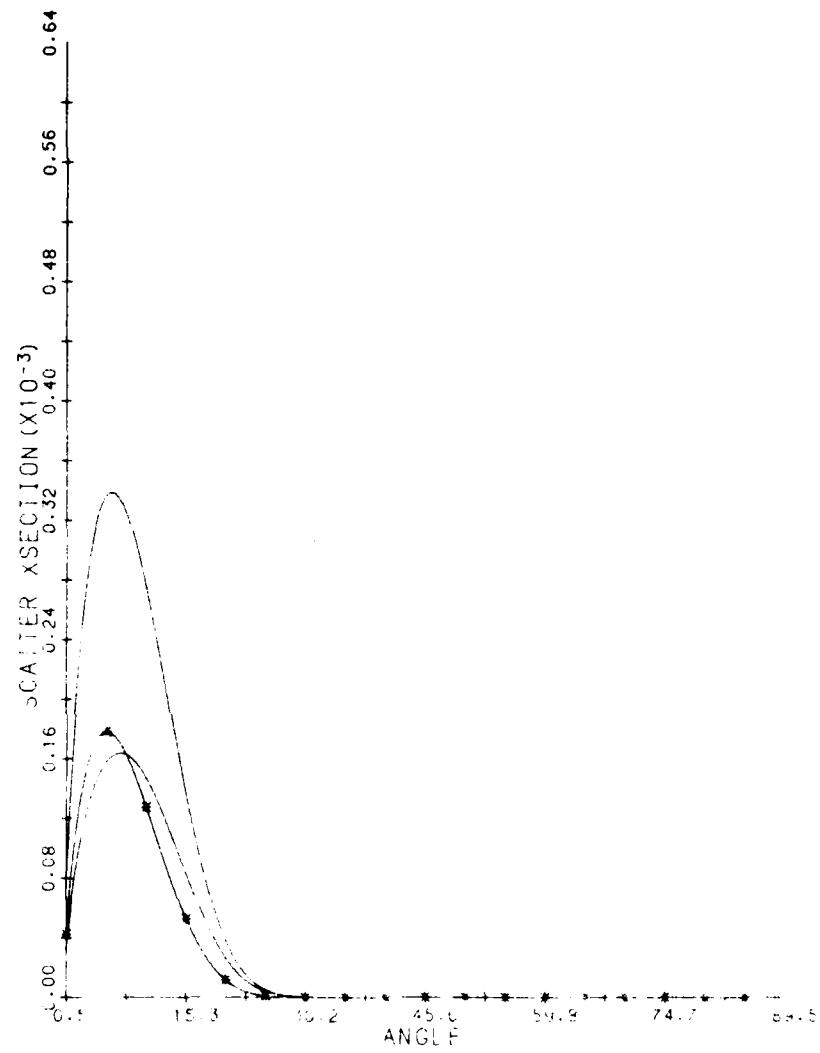
Figure 11a. Plot of Modified Born, Multi-scattering, and Total
Cross Section as a Function of χ_1 for: $\chi_1 = 0$, $n = 4$,
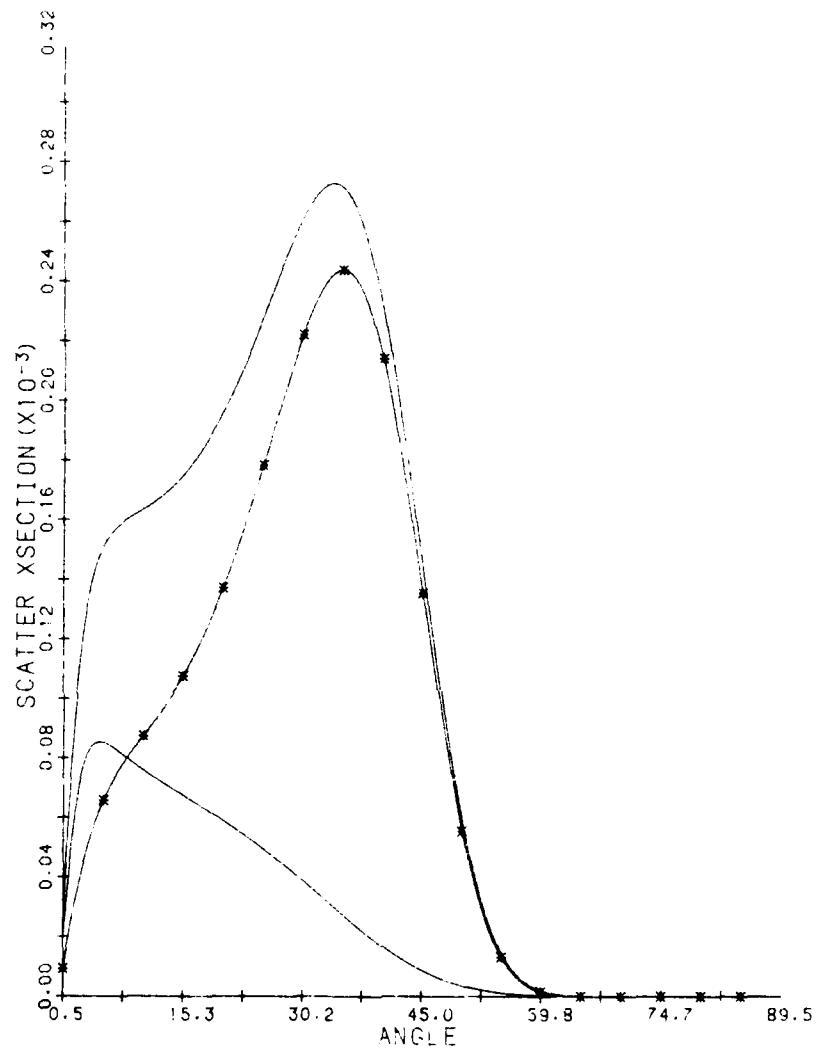$L = 10000$, $\lambda = 0.8$
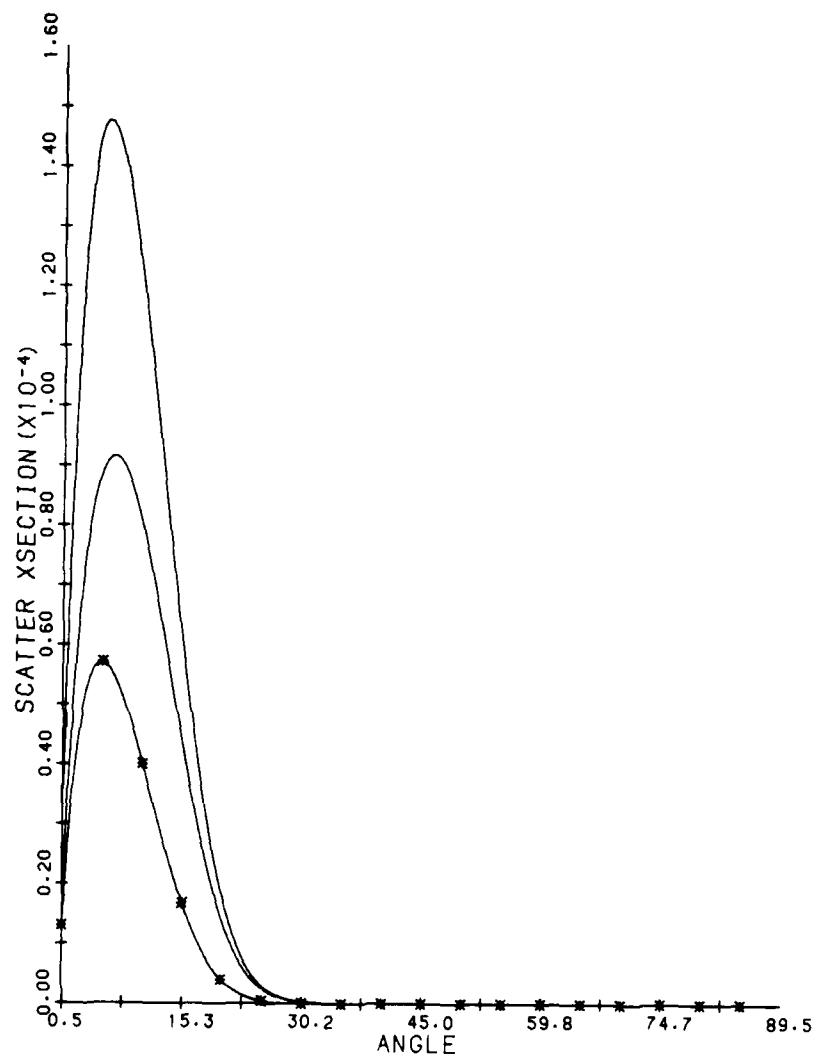
Figure 11b. Plot of Modified Born, Multiscattering, and Total
Cross Section as a Function of λ_f for: $\lambda_i = 15^o$, $\eta = 4$,
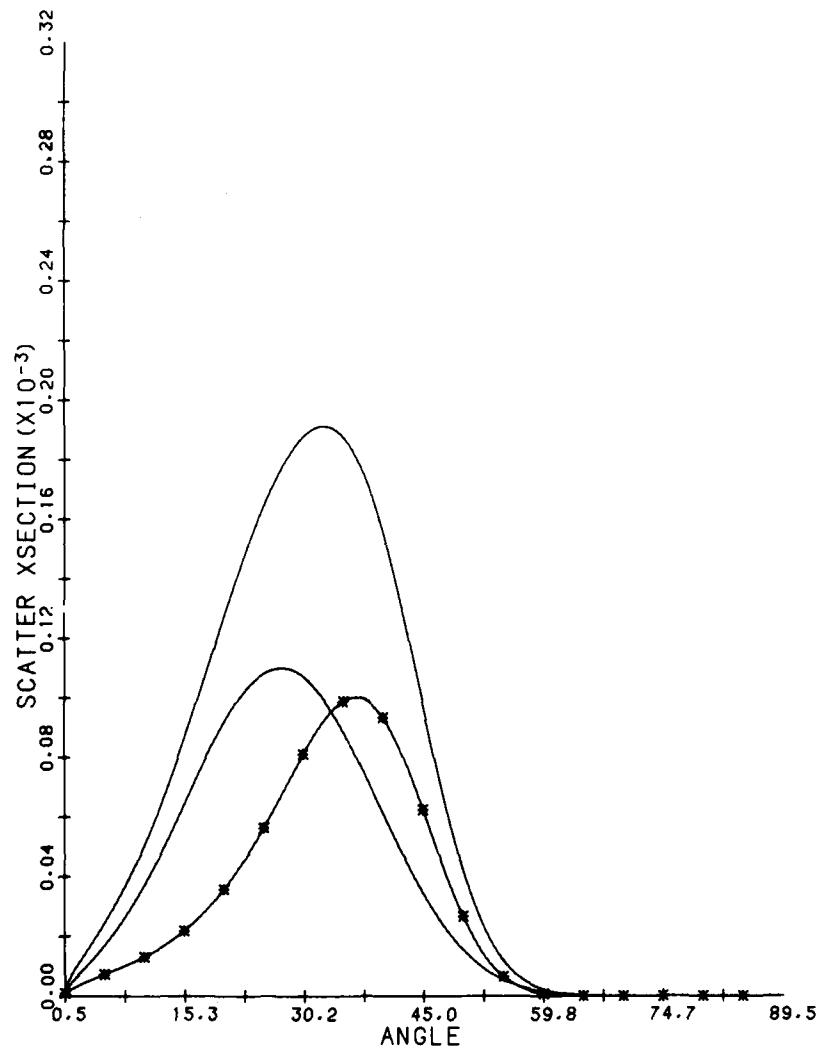L = 10000, $\lambda = 0.8$
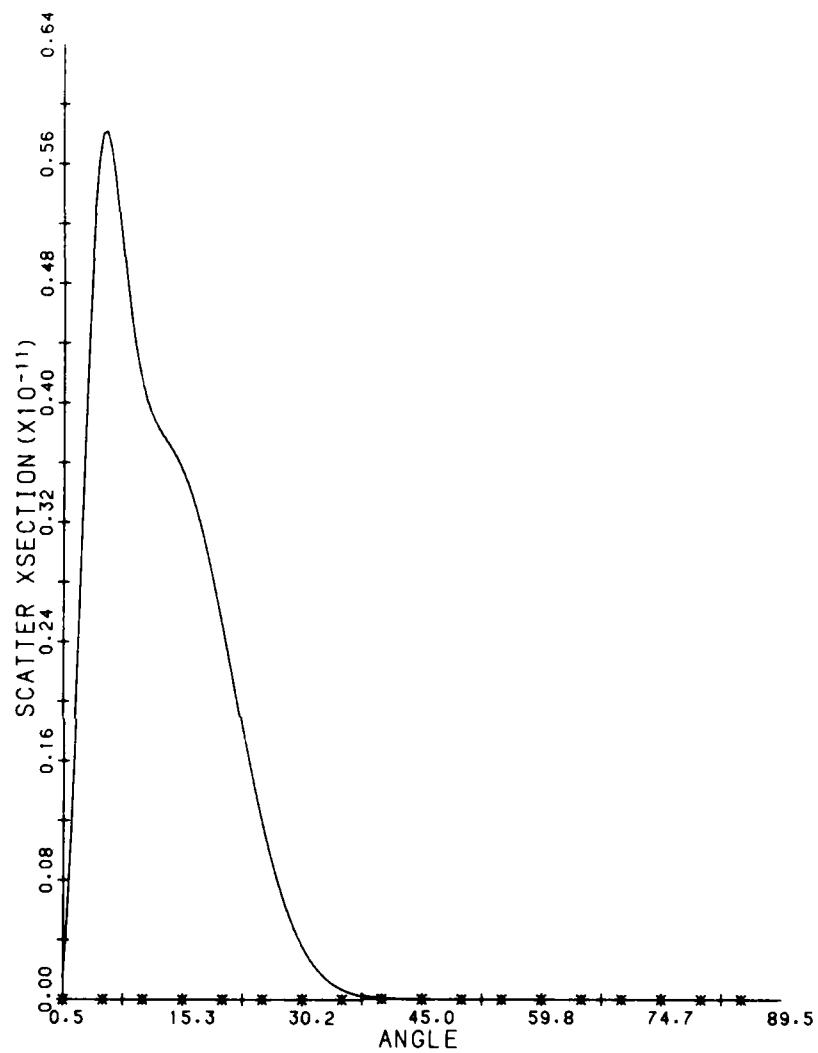
Figure 11c. Plot of Modified Born, Multiscattering, and Total Cross Section as a Function of χ_f for: $\chi_i = 45°$, $\eta = 4$, $L = 10000$, $\lambda = 0.8$
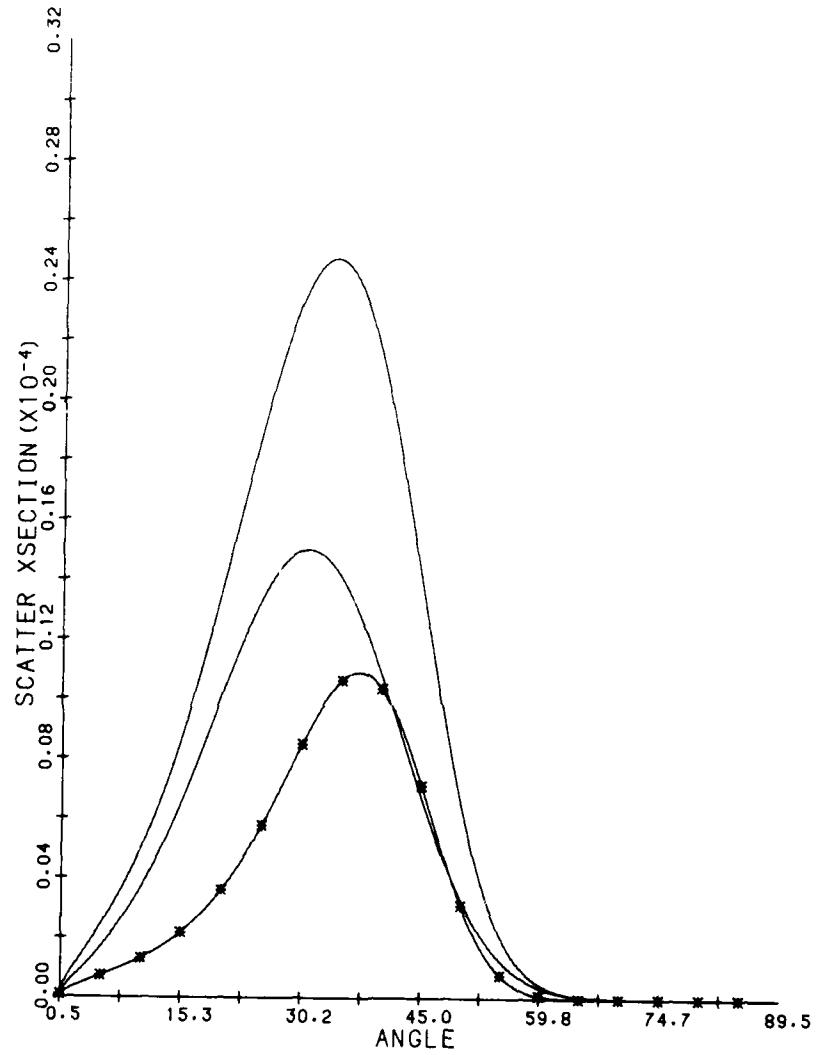
62
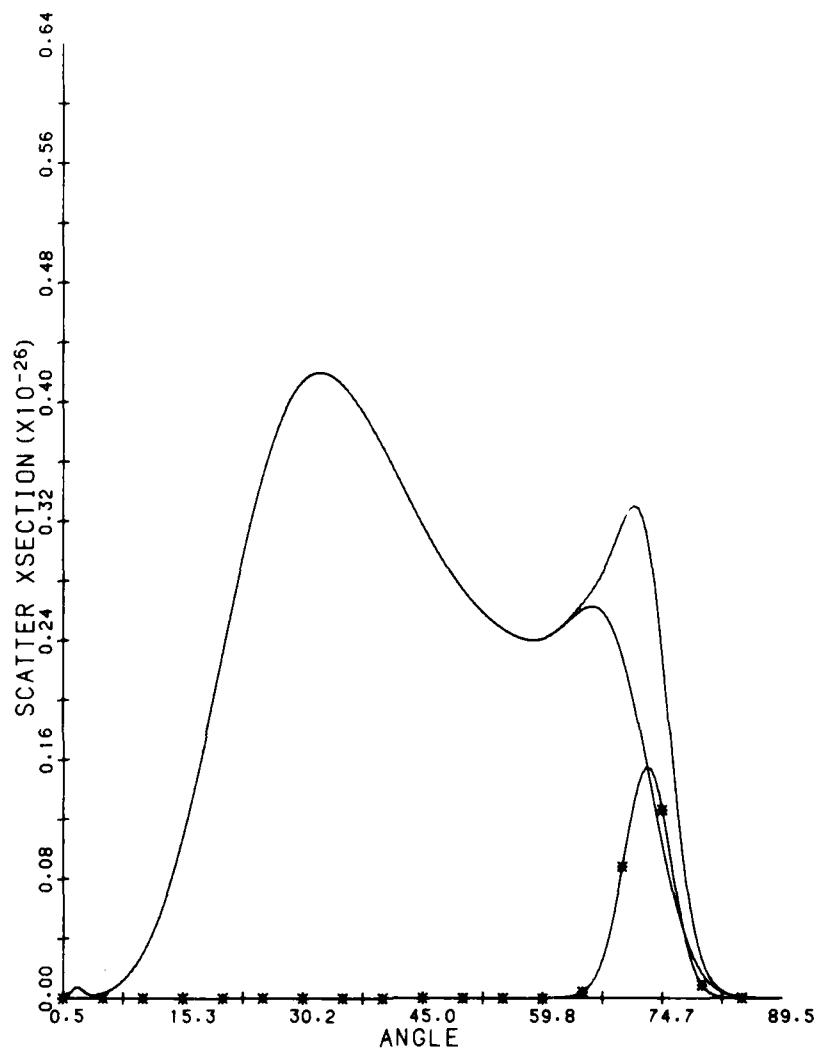
Figure 11d. Plot of Modified Born, Multiscattering, and Total Cross Section as a Function of χ_f for: $\chi_i = 75^\circ$, $\eta = 4$, $L = 10000$, $\lambda = 0.8$
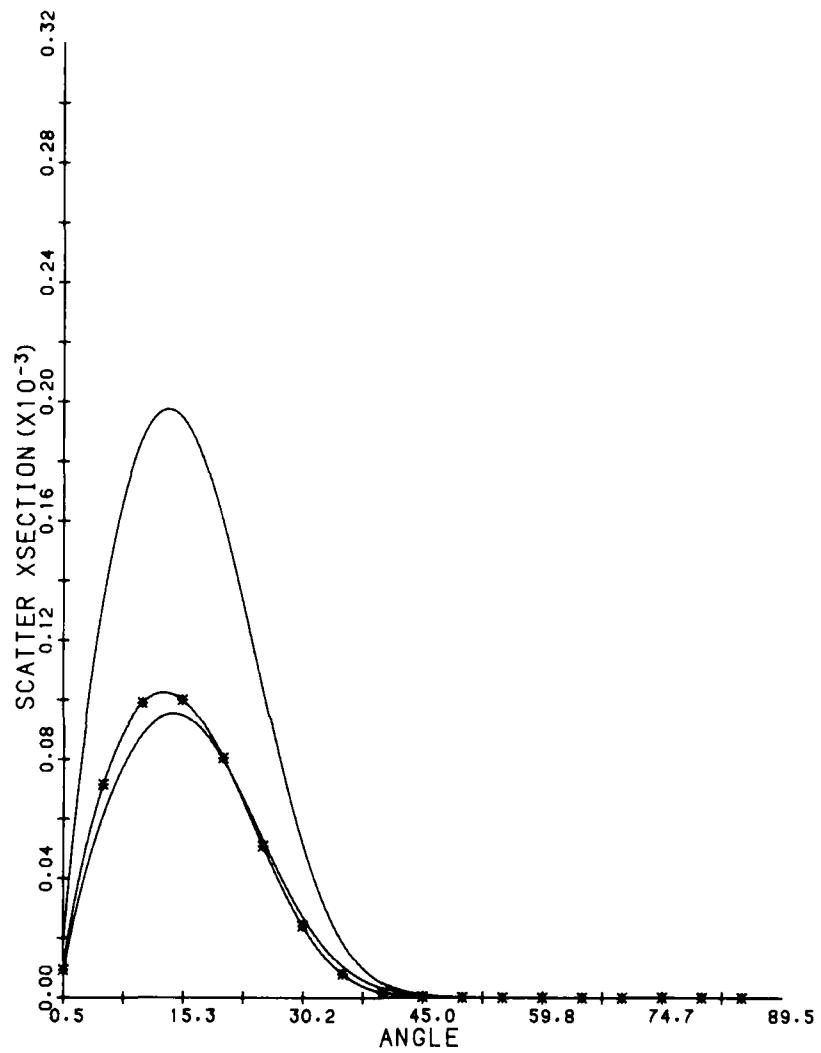
63
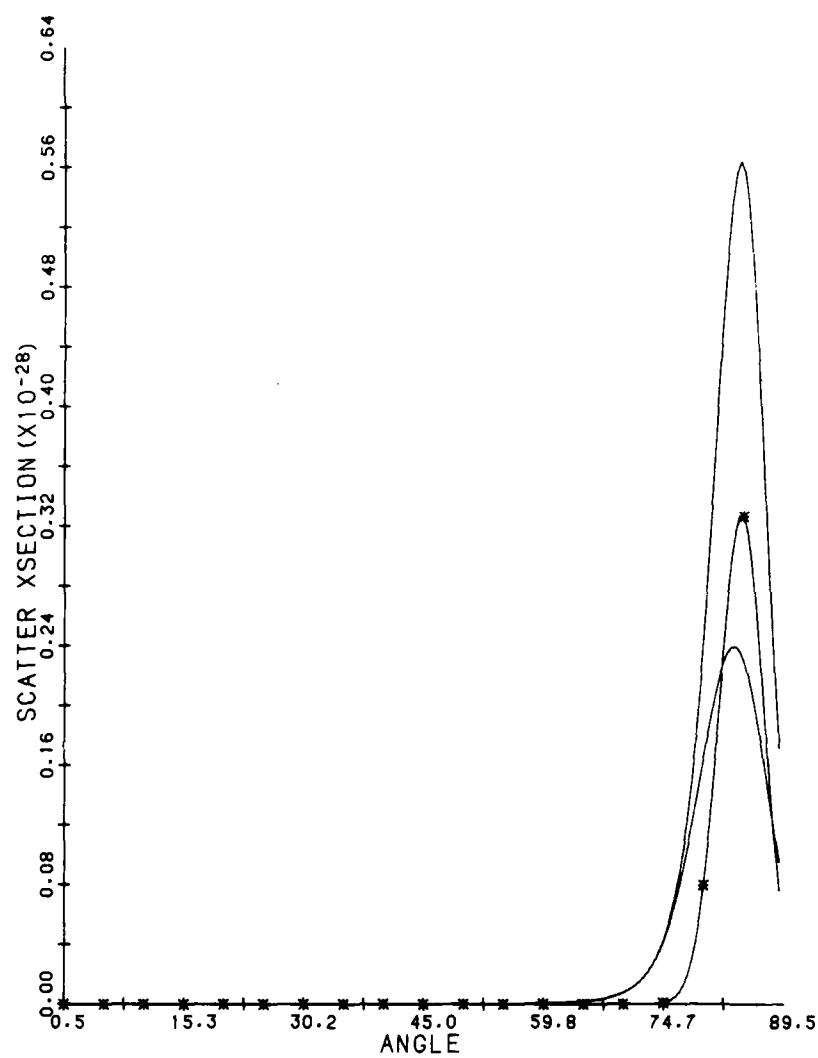
Figure 11e. Plot of Modified Born, Multiscattering, and Total Cross Section as a Function of χ_f for: $\chi_i = 85^o$, $\eta = 4$, $L = 10000$, $\lambda = 0.8$

64

References

1. Haerendel, G., Lust, R. and Rieger, E. (1967) Motion of artificial ion clouds in the upper atmosphere, Planet Space Sci. 1:1.

2. Perkins, F.W., Zabusky, N.J., and Doles III, J.H. (1973) Deformation and striation of plasma clouds in the ionosphere, 1, J. Geophys. Res. 78: 5.

3. Utlaut, A.F., and Cohen, R. (1971) Modifying the ionosphere with intense Radio Waves, Science 174:245.

4. Rao, P.B., and Thome, G.D. (1974) A model for RF scattering field-aligned heater-induced irregularities, Radio Sci. 9:987.

5. DeWolf, D.A. (1971) Electromagnetic reflection from an extended turbulent medium: Cumulative forward-scatter single-backscatter approximation, IEEE Trans. Antenna Propag. AP 19:254.

6. Fradkin, E.S. (1966) Application of functional methods in quantum field theory and quantum statistics (II), Nucl. Phys. 76:588.

7. Kubo, R. (1962) Generalized cumulant expansion method, J. Phys. Soc. Japan 17:1100.

8. Bendow, B., Yukon, S.P., and Ying, S.C. (1974) Theory of multiphonon absorption due to nonlinear electric moments in crystals, Phys. Lett. 49A:229.

9. Tatarskii, V.I. (1971) The effect of the turbulent atmosphere on wave propagation, Israel Program for Scientific Translations, Jerusalem.

10. Mitekhin, G.V. (1965) The infrared asymptotic behavior of the Green's function in some models of quantum field theory, Sov. Phys. -JETP 1:271.

Appendix A

Calculation of Effective Path Length

The path length AC may be determined in terms of the polar and azimuth angles χ, ϕ of the ray direction $\hat{K}$, and the distance into the medium x by

$$AC = (AB^2 + BC^2)^{1/2} \quad , \tag{A1}$$

where

$$x = BD, \quad AB = x \tan (\phi), \quad \text{and} \quad BC = x/\sin (\chi) \tag{A2}$$

as indicated in Figure A1.
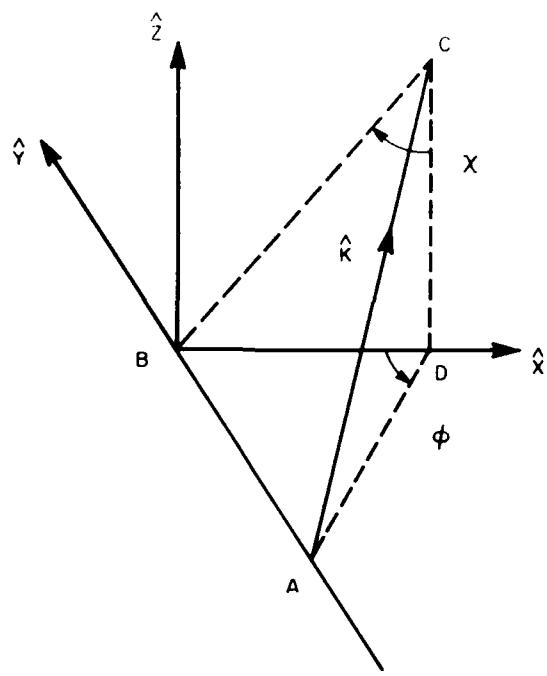
Figure A1. Geometry for Determining Effective
Path Length for a Given Scattering Wave Vector

Appendix B

Evaluation of $\partial_f^n [e^f - 1]/f$ in Terms of the Incomplete Gamma Function

The nth derivative of $(e^f - 1)/f$ with respect to f may be reexpressed by using the Leibniz theorem as

$$\partial^n \left[\frac{e^f - 1}{f} \right] = \partial^n \left[\frac{e^f}{f} \right] - \partial^n \left[\frac{1}{f} \right]$$

$$= \left[(\partial^n e^f)(f^{-1}) + \binom{n}{1}(\partial^{n-1} e^f)(\partial f^{-1}) \right.$$

$$\left. + \binom{n}{2}(\partial^{n-2} e^f)(\partial^2 f^{-1}) + \cdots + e^f \partial^n (f^{-1}) \right] - \partial^n (f^{-1}) \quad . \tag{B1}$$

Using

$$\partial(f^{-1}) = (-1)f^{-2} \quad , \quad \partial^2(f^{-1}) = (-1)(-2)f^{-3}, \quad \cdots \partial^n(f^{-1}) = (-1)(-2)\cdots(-n) f^{-n-1} \tag{B2}$$

this becomes

$$\frac{e^f}{f}\left[1 + \binom{n}{1}(-f^{-1}) + \binom{n}{2}2!\,(-f^{-1})^2 + \cdots + \binom{n}{j}j!\,(-f^{-1})^j\right.$$

$$\left.+ \cdots + n!\,(-f^{-1})^n\right] - n!\,\frac{(-f^{-1})^n}{f} \quad , \tag{B3}$$

thus

$$\frac{\partial^n\left[\dfrac{e^f - 1}{f}\right]}{n!} = \frac{e^f}{f}\sum_{j=0}^{n}\binom{n}{j}(-f^{-1})^j\,\frac{j!}{n!} - \frac{(f^{-1})^n}{f}$$

$$= \frac{e^f}{f}\sum_{j=0}^{n}\frac{1}{(n-j)!}(-f^{-1})^j - \frac{(-f^{-1})^n}{f} \quad . \tag{B4}$$

Letting $k = n - j$ this can be reexpressed as

$$\frac{e^f}{f}\sum_{k=n}^{0}\frac{1}{k!}(-f^{-1})^{n-k} - \frac{(-f^{-1})^n}{f} = \frac{e^f}{f}(-f^{-1})^n\sum_{k=0}^{n}\frac{1}{k!}(-f)^k - \frac{(-f^{-1})^n}{f}$$

$$= \frac{(-1)^n}{f^{n+1}}\left\{e^f\sum_{k=0}^{n}\frac{(-f)^k}{k!} - 1\right\} \quad . \tag{B5}$$

Evaluating this at the point $f = -x$ yields

$$\partial^n\left[\frac{e^f - 1}{f}\right]_{f=-x} = \frac{-n!}{x^{n+1}}\left[e^{-x}\sum_{k=0}^{n}\frac{x^k}{k!} - 1\right] \quad . \tag{B6}$$

The series expansion for the incomplete gamma function is given by

$$\gamma(n + 1,\ x) = n!\left(1 - e^{-x}\sum_{k=0}^{n}\frac{x^k}{k!}\right) \quad . \tag{B7}$$

Thus,

$$\partial^n \left[\frac{e^f - 1}{f} \right]_{f=-x} = \frac{\gamma(n + 1, \ x)}{x^{n+1}} \qquad . \tag{B8}$$

71

Appendix C

Convolution of Projected Correlation Functions

To show that the convolution of two projected correlation functions is another projected correlation function we start from the definition of $\overset{\vee}{D}{}^n_j(\vec{p}_\perp)$ in Eq. (56), where $\overset{\vee}{D}_i(\vec{p}_\perp)$ is defined in the plane $p_x - p_y$ perpendicular to $\vec{p}_z$ at the origin $(p_z = 0)$,

$$\widetilde{D}_i(\vec{p}) = \overset{\vee}{D}_i(\vec{p}_\perp)[2\pi\delta(\vec{p} \cdot \vec{K})K_z]$$

$$= \overset{\vee}{D}_i(\vec{p}_\perp)2\pi\delta\left(p_z + \frac{\vec{K}_\perp \cdot \vec{p}_\perp}{K_z}\right).$$

(C1)

The convolution of $\widetilde{D}_i$ with $\widetilde{D}_i$ to yield $\widetilde{D}^2_i$ is defined in Eq. (51) and yields, using the expression C1 for $\widetilde{D}_i(\vec{p})$,

$$\widetilde{D}^2_i(\vec{Q}) = \int \frac{d\vec{p}}{(2\pi)^3} \widetilde{D}_i(\vec{Q} - \vec{p})\widetilde{D}_i(\vec{p})$$

$$= \int \frac{d\vec{p}_\perp}{(2\pi)^3} \overset{\vee}{D}_i(\vec{Q}_\perp - \vec{p}_\perp)\overset{\vee}{D}_i(\vec{p}_\perp)2\pi\delta\left(p_z + \frac{\vec{p}_\perp \cdot \vec{K}_{i\perp}}{K_{iz}}\right)$$

73

$$\times 2\pi\delta\left(Q_z - p_z + \frac{\vec{K}_{i\perp}\cdot(\vec{Q}_\perp - \vec{p}_\perp)}{K_{iz}}\right)dp_z$$

$$= 2\pi\delta\left(Q_z + \frac{\vec{K}_{i\perp}\cdot\vec{Q}_\perp}{K_{iz}}\right)\check{D}_i^2(\vec{Q}_\perp)$$

$$= \check{D}_i^2(\vec{Q}_\perp)\left[2\pi\delta(\vec{Q}\cdot\vec{K})K_z\right]$$

$$= \widetilde{D}_i^2(\vec{Q}) \tag{C2}$$

Higher order convolutions follow from Eq. (51).

Appendix D

Multiscattering Term for Gaussian Correlation Function

The general term of Eq. (61) can be written using the factored Gaussian of Eq. (57) and the coordinate system of Figure 3 as

$$\mathscr{L}^{nj} \equiv \frac{1}{(2\pi)^6} \iint d\vec{q}\, d\vec{p}\, \widetilde{\Phi}_{\mathcal{D}}(\vec{p} - \vec{q})\, \overset{\vee}{D}_i^{n-j}(\vec{p}_\perp - \vec{K}_{i\perp})\, \overset{\vee}{D}_f^j(\vec{q}_\perp - \vec{K}_{f\perp})\delta((\vec{p} - \vec{K}_i)\cdot\vec{K}_i)$$

$$\times\ \delta((\vec{q} - \vec{K}_f)\cdot\vec{K}_f)[2\pi K_{iz}]\,[2\pi K_{fz}]$$

$$= \frac{1}{(2\pi)^6}\, \frac{\int d\vec{q}_\perp \int d\vec{p}_\perp}{[K_{iz}\, K_{fz}]}\, \widetilde{\mathscr{D}}(\vec{p}_\perp - \vec{q}_\perp)\, \widetilde{\mathscr{D}}_i^{n-j}(\vec{p}_\perp - \vec{K}_{i\perp})\, \widetilde{\mathscr{D}}_f^j(\vec{q}_\perp - \vec{K}_{f\perp})$$

$$\times\ \widetilde{d}\left(\left[\frac{\vec{K}_{i\perp}\cdot(\vec{p}_\perp - \vec{K}_{i\perp}) - K_{iz}^2}{K_{iz}}\right] - \left[\frac{\vec{K}_{f\perp}\cdot(\vec{q}_\perp - \vec{K}_{f\perp}) - K_{fz}^2}{K_{fz}}\right]\right)$$

$$\times\ \widetilde{d}_i^{n-j}\left(\left[\frac{\vec{p}_\perp\cdot\vec{K}_i - \vec{K}_{i\perp}^2}{K_{iz}}\right]\right)\widetilde{d}_f^j\left(\left[\frac{\vec{q}_\perp\cdot\vec{K}_{f\perp} - \vec{K}_{f\perp}^2}{K_{fz}}\right]\right)(2\pi)^2\, K_{iz}\, K_{fz}\quad,$$

$$\tag{D1}$$

75

where we have used the two projection delta functions to integrate over q_z and p_z. The argument of $\widetilde{\mathscr{D}}\,(\vec{p}_\perp - \vec{q}_\perp)$ may be expressed using Eq. (62) and letting $s = \sin(\phi_f - \phi_i)$, $c = \cos(\phi_f - \phi_i)$ as

$$\left| \left[\vec{q}_\perp - \vec{p}_\perp \right]_{\text{along } \hat{p}_1} \right|^2 = [-q_2 s + q_1 c - p_1]^2 \tag{D2}$$

$$\left| \left[\vec{q}_\perp - \vec{p}_\perp \right]_{\text{along } \hat{p}_2} \right|^2 = [q_1 s + q_2 c - p_2]^2 \tag{D3}$$

$$\left[\vec{q}_\perp - \vec{p}_\perp \right]^2 = q_1^2 + q_2^2 - 2p_1(q_1 c - q_2 s) - 2p_2(q_1 s + q_2 c) + p_1^2 + p_2^2 \quad . \tag{D4}$$

This yields

$$\mathscr{L}^{nj} = \frac{1}{(2\pi)^4} \left[\frac{\pi L_\perp \widetilde{L}_i}{(n-j)} \right] \left[\frac{\pi L_\perp \widetilde{L}_f}{(j)} \right] \left[\frac{\pi L_\perp^2 \sqrt{\pi}\, L_{\parallel}}{1} \right] \times$$

$$\times \iint dp_1 \, dq_1 \; e^{-(p_1 - K_{i\perp})^2 \widetilde{L}_i^2 / 4(n-j)} \; e^{-(q_1 - K_{f\perp})^2 \widetilde{L}_f^2 / 4j}$$

$$\times \; e^{-[(p_1 - K_{i\perp})\tan\chi_i - K\cos\chi_i - (q_1 - K_{f\perp})\tan\chi_f + K\cos\chi_f]^2 L_{\parallel}^2 / 4}$$

$$\times \iint dp_2 \, dq_2 \; e^{-(p_2 - K_{i2})^2 L_\perp^2 / 4(n-j)} \; e^{-(q_2 - K_{f2}) L_\perp^2 / 4j}$$

$$\times \; e^{-\left[q_1^2 + p_1^2 - 2p_1 q_1 c \right] L_\perp^2 / 4} \; \times \; e^{-\left[q_2^2 + p_2^2 - 2p_2(q_1 s + q_2 c) + 2p_1 q_2 s \right] L_\perp^2 / 4}$$

$$\tag{D5}$$

Performing the integration over p_2 and q_2 gives

$$\int dp_2 \int dq_2 \, e^{-p_2^2 L_\perp^2/4(n-j)} \, e^{-q_2^2 L_\perp^2/4j}$$

$$\times \, e^{-\left[q_2^2+p_2^2-2p_2(q_1 s+q_2 c)+2p_1 q_2 s\right] L_\perp^2/4}$$

$$= \frac{4\pi}{L_\perp^2} \left[\frac{j(n-j)}{1+n+js^2(n-j)}\right]^{1/2} e^{+p_1^2 s^2 L_\perp^2/4(1+1/j)}$$

$$\times e^{[-q_1 s+p_1 s\cdot c/(1+1/j)]^2/\mathscr{P}_o^2} \quad , \tag{D6}$$

where

$$\mathscr{P}_o = [(n+1)+js^2(n-j)]/[(n-j)(j+1)] \quad . \tag{D7}$$

Performing the p_1, q_1 integration then yields

$$\mathscr{L}^{nj} = \frac{\sqrt{\pi}}{4} \frac{\widetilde{L}_i \widetilde{L}_f L_\parallel}{\sqrt{n+1+j(n-j)s^2}} \frac{1}{\sqrt{j(n-j)}} \frac{\pi}{\sqrt{\alpha_2 \beta_2 + \gamma^2/4}}$$

$$\times e^{[\alpha_1+\beta_1 \gamma/2\beta_2]^2/4[\alpha_2+\gamma^2/4\beta_2]} e^{\beta_1^2/4\beta_2} e^{\Gamma} \quad , \tag{D8}$$

where

$$\alpha_1 = \frac{1}{2}\left\{-x_1 + cy_1 + \eta^2(x_o t_o^2 - y_o t_o t_s) + \frac{s^2 x_1}{(1+1/j)} + \frac{c^2 s^2 x_1}{\mathscr{P}_o^2(1+1/j)}\right.$$

$$\left. - \frac{c s^2 y_1}{\mathscr{P}_o^2(1+1/j)}\right\}$$

$$\alpha_2 = \frac{1}{4}\left\{\frac{\eta_o^2}{(n-j)} + (\eta^2 t_o^2 + 1) - \frac{s^2}{(1+1/j)} - \frac{c^2 s^2}{\mathscr{P}_o^2(1+1/j)^2}\right\}$$

$$\beta_1 = \frac{1}{2}\left\{-y_1 + x_1 + n^2(x_0 t_s^2 - x_0 t_0^2) + \cdots \right.$$

$$\beta_2 = \frac{1}{4}\left\{\frac{ns^2}{j} + \left[n^2 t_s^2 + 1\right] - \frac{s^2}{\rho_o^2} \right.$$

$$\gamma = \frac{1}{2}\left\{n^2 t_0 t_s + c - \frac{c s^2}{\rho_o^2(1 + 1/j)} \right.$$

$$\Gamma = \frac{1}{4}\left\{-(x_1^2 + y_1^2) - (x_0^2 n^2 t_0^2 + y_0^2 n^2 t_s^2)\right.$$

$$+ 2x_0 y_0 n^2 t_0 t_s + 2x_1 y_1 c + \frac{s^2 x_1^2}{(1 + 1/j)}$$

$$+ \frac{s^2 y_1^2}{\rho_o^2} + \frac{c^2 s^2 x_1}{\rho_o^2(1 + 1/j)^2} - \frac{2 c s^2 x_1 y_1}{\rho_o^2(1 + 1/j)}\right\} \tag{D9}$$

with

$$\eta = \frac{L_\parallel}{L_\perp} \quad , \quad \eta_o = \frac{\widetilde{L}_i}{L_\perp} \quad , \quad \eta_s = \frac{\widetilde{L}_f}{L_\perp}$$

$$\widetilde{L}_i^2 = L_\perp^2 + L_\parallel^2 \tan^2(\chi_i) \quad , \quad \widetilde{L}_f^2 = L_\perp^2 + L_\parallel^2 \tan^2(\chi_f)$$

$$x_0 = K \cos^2(\chi_i) L_\perp / \sin \chi_i \quad , \quad x_1 = K_{o\perp} L_\perp$$

$$y_0 = K \cos^2(\chi_f) L_\perp / \sin \chi_f \quad , \quad y_1 = K_{f\perp} L_\perp \quad . \tag{D10}$$

78

Appendix E

Multiscattering Term for Gaussian Correlation Function for $j = 0$, $n - j > 0$

The general term of the sum of Eq. (54) with $n' = (n - j) > 0$, $j = 0$ or with an interchange of subscripts $i \longleftrightarrow f$ for $(n - j) = 0$, $j > 0$) can be written for the Gaussian correlation function as

$$\mathscr{L}^{n'} = \int e^{i \Delta \vec{K} \cdot \Delta \vec{r}} \, \Phi_{\mathscr{Y}}(\Delta \vec{r}) \, D_i^{n'}(\Delta \vec{r}) \, d\Delta \vec{r}$$

$$= \int d\Delta \vec{r} \, e^{i(\vec{K}_i - \vec{K}_f) \cdot \Delta \vec{r}} \int \frac{d\vec{p}}{(2\pi)^3} \, e^{i \vec{p} \cdot \Delta \vec{r}} \, \tilde{\Phi}_{\mathscr{Y}}(\vec{p})$$

$$\times \int \frac{d\vec{q}}{(2\pi)^3} \, e^{-i \vec{q} \cdot \Delta \vec{r}} \, \overset{\vee}{D}_i^{n'}(\vec{q}_\perp) \delta(\vec{q} \cdot \vec{K}_i) \{2\pi K_{iz}\}$$

$$= \frac{1}{(2\pi)^3} \int d\vec{p} \int d\vec{q} \, \tilde{\Phi}_{\mathscr{Y}}(\vec{p}) \, \overset{\vee}{D}_i^{n'}(\vec{q}_\perp) \cdot \delta(\vec{q} \cdot \vec{K}_i)$$

$$\times \delta(\vec{K}_i - \vec{K}_f + \vec{p} + \vec{q}) \{2\pi K_{iz}\}$$

$$= \frac{1}{(2\pi)^3} \int d\vec{q}\, \widetilde{\Phi}_{\mathcal{Y}} (\vec{q} + \vec{K}_i - \vec{K}_f) \overset{\vee}{D}_i^{n'}(\vec{q}_\perp) \delta(\vec{q} \cdot \vec{K}_i) [2\pi K_{iz}] \quad . \qquad (\text{E1})$$

Letting $\vec{q}' = \vec{q} + \vec{K}_i$ and dropping primes, this may be written as

$$\mathcal{L}^{n'} = \frac{1}{(2\pi)^3} \int d\vec{q}\, \widetilde{\Phi}_{\mathcal{Y}} (\vec{q} - \vec{K}_f) \overset{\vee}{D}_i^{n'}(\vec{q} - \vec{K}_i) \delta((\vec{q} - \vec{K}_i) \cdot \vec{K}_i) [2\pi K_{iz}] \quad . \qquad (\text{E2})$$

Taking the $\hat{q}_{\perp 1}$ axis along $\vec{K}_{\perp i}$ yields

$$\left\{ \vec{K}_{f\perp} \right\}_{\text{along } q_1} = K_{f\perp} \cos(\phi_f - \phi_i) \qquad (\text{E3})$$

$$\left\{ \vec{K}_{f\perp} \right\}_{\text{along } q_2} = K_{f\perp} \sin(\phi_f - \phi_i) \qquad (\text{E4})$$

hence

$$\vec{K}_{f\perp} - \vec{q}_\perp = \left[K_{f\perp} \cos(\phi_f - \phi_i) - q_1 \right] \hat{q}_1 + \left[K_{f\perp} \sin(\phi_f - \phi_i) - q_2 \right] \hat{q}_2 \qquad (\text{E5})$$

and $\mathcal{L}^{n'}$ may be written as

$$\mathcal{L}^{n'} = \int \frac{d\vec{q}_\perp}{(2\pi)^3 K_{iz}} \widetilde{\mathcal{D}} (\vec{K}_{f\perp} - \vec{q}_\perp) \widetilde{\mathcal{D}}_i^{n'}(\vec{q}_\perp - \vec{K}_{i\perp}) [2\pi K_{iz}]$$

$$\times \widetilde{d} \left(K_{fz} + \frac{(\vec{q}_\perp \cdot \vec{K}_{i\perp} - K^2)}{K_{iz}} \right) \widetilde{d}_i^{n'} \left(- \frac{(\vec{q}_\perp \cdot \vec{K}_{i\perp} - K^2)}{K_{iz}} - K_{iz} \right) \quad .$$

$$(\text{E6})$$

80

Letting $c = \cos(\phi_f - \phi_i)$ and $s = \sin(\phi_f - \phi_i)$ this may be written as

$$
\mathscr{L}^{n'} = \int \frac{d\vec{q}_\perp}{(2\pi)^3 K_{iz}} \left[\frac{\pi L_\perp^2}{1} \cdot \frac{\sqrt{\pi} L_\parallel}{1} \cdot \frac{\pi L_\perp \tilde{L}_i}{n'} \right] \lfloor 2\pi K_{iz} \rfloor
$$

$$
\times \ e^{-(K_{f\perp} \cdot c - q_1)^2 L_\perp^2 / 4} \ e^{-(K_{f\perp} s - q_2)^2 L_\perp^2 / 4}
$$

$$
\times \ e^{-(q_1 - K_{i\perp})^2 \tilde{L}_i^2 / 4n'} \ e^{-(q_2)^2 L_\perp^2 / 4n'}
$$

$$
\times \ e^{-\left(K_{fz} + \frac{\vec{q}_\perp \cdot \vec{K}_{i\perp} - K^2}{K_{iz}} \right)^2 L_\parallel^2 / 4} \quad , \tag{E7}
$$

Carrying out the indicated integration this becomes

$$
\mathscr{L}^{n'} = \frac{\pi \sqrt{\pi} L_\perp^2 L_\parallel}{(n'+1)} \ e^{-\frac{1}{4}\left[\frac{y_1^2 s^2}{(n'+1)} + (x_1 - y_1 c)^2 \right]}
$$

$$
\times \ e^{-\frac{1}{4}(x_a - y_a)^2 \eta^2} \ e^{\frac{1}{4\mathscr{P}_i^2}[(x_1 - y_1 c) - (x_a - y_a)\eta^2 \tan(\chi_i)]^2} \tag{E8}
$$

where

$$
x_1 = K_{i\perp} L_\perp \qquad , \qquad y_1 = K_{f\perp} L_\perp \quad ,
$$

$$
x_a = K \cos(\chi_i) L_\perp \qquad , \qquad y_a = K \cos(\chi_f) L_\perp \quad ,
$$

$$
\tilde{L}_i = \left[L_\perp^2 + L_\parallel^2 \tan^2(\chi_i) \right]^{1/2} \quad ,
$$

$$
\eta_i = \tilde{L}_i / L_\perp \quad ,
$$

and where

$$
\mathscr{P}_i = [1 + \eta_i / n' + \eta^2 \tan^2(\chi_i)]^{1/2} \quad . \tag{E10}
$$

Representation of Kolmogoroff Correlation Function by
a sum of Gaussians

In order to approximate $D_f^B(\vec{\eta})$ as a sum of separable Gaussians, we assume
that it can be represented in a form similar to $D_{\chi\chi}(\vec{\eta})$, where from Eq. (6.5) we

$$D_{\chi\chi}^B(\vec{\eta}) = \sum_{i=1}^{N} (1)_i e^{-\pi^2 \mu_1^2 \eta^2 \sigma_i^2}$$

$$= \check{D}_f^1(\vec{\eta}) \frac{1}{\left[1 + \frac{\eta^2}{L_0^2} \right]^{-1 + \mu}} e^{-\pi^2 \eta^2 (\nu_1) \sigma_i^2} \qquad (1)$$

where

$$(1)_i = \frac{\nu_i x_i^{\mu}}{\Gamma(\mu + 1)} \qquad \sigma_i = x_i L_0^2 \qquad (2)$$

$$\sigma_i = \nu_i \pi^{-1} \cot^{-1}\left(-\nu^{-1/2}/4\right) \qquad (3)$$

with w_i and x_i the Gauss-Laguerre weights and zeros. We are thus led to assume a form for $\overset{v}{D}{}^n_{Af}$ given by

$$\overset{v}{D}{}^n_{Af}(\vec{p}_\perp) = \sum_{i=1}^{M} c_i^{(n)} \, e^{-\alpha_i^{(n)} p_2^2 - \beta_i^{(n)} p_1^2} \quad , \tag{F4}$$

where in analogy to the Gaussian case we take

$$\alpha_i^{(n)} = \alpha_i/n \quad , \qquad \beta_i^{(n)} = \beta_i/n \quad . \tag{F5}$$

To determine the optimum $C_2^{(n)}$ we follow Shavitt[F1] and minimize the deviation $\Delta^{(n)}$ given by

$$\Delta^{(n)} = \int \left[\int \overset{v}{D}{}^{n-1}_{Af}(\vec{Q}_\perp - \vec{p}_\perp) \overset{v}{D}{}^1_f(\vec{p}_\perp) \, d\vec{p}_\perp - \sum_{i=1}^{M} C_i^{(n)} e^{-\left[\alpha_i Q_2^2 + \beta_i Q_1^2\right]/n} \right]^2 \times$$

$$\times \, W(\vec{Q}_\perp) d\vec{Q}_\perp \tag{F6}$$

where $W(\vec{Q}_\perp)$ is an arbitrary weight function. Minimizing $\Delta^{(n)}$ leads to the set of equations

$$\frac{\partial \Delta^{(n)}}{\partial C_i^{(n)}} = \sum_{j=0}^{M} 2 C_j^{(n)} \, A_{ij}^{(n)} \quad , \tag{F7}$$

where

$$A_{ij}^{(n)} = \int G_i^{(n)}(\vec{p}_\perp) G_j^{(n)}(\vec{p}_\perp) W(\vec{p}_\perp) \, d\vec{p}_\perp \tag{F8}$$

$$A_{in}^{(n)} = - \int G_i^{(n)}(\vec{p}_\perp) g^{(n)}(\vec{p}_\perp) W(\vec{p}_\perp) \, d\vec{p}_\perp \tag{F9}$$

F1. Shavitt, I. (1963) Methods in Computational Physics, B. Alder, S. Fernbach, and M. Rotenberg, Eds., Vol. 2, Academic Press, N.Y.

with

$$G_i^{(n)}(\vec{p}_\perp) = e^{-(\alpha_i p_2^2 + \beta_i p_1^2)/n} \tag{F10}$$

and

$$g^{(n)}(\vec{p}_\perp) = \int \frac{d\vec{p}_\perp}{(2\pi)^2} \; \overset{\vee}{D}_{Af}^{n-1}(\vec{p}_\perp) \; \overset{\vee}{D}_f^1(\vec{p}_\perp) \quad . \tag{F11}$$

The set of M simultaneous linear equations given by Eq. (F7) can then be solved for $C_i^{(n)}$.

MISSION
of
Rome Air Development Center

RADC plans and executes research, development, test and selected acquisition programs in support of Command, Control Communications and Intelligence (C^3I) activities. Technical and engineering support within areas of technical competence is provided to ESD Program Offices (POs) and other ESD elements. The principal technical mission areas are communications, electromagnetic guidance and control, surveillance of ground and aerospace objects, intelligence data collection and handling, information system technology, ionospheric propagation, solid state sciences, microwave physics and electronic reliability, maintainability and compatibility.

END

FILMED

6-83

DTIC